HHS Public Access

Author manuscript

Dev Neurobiol. Author manuscript; available in PMC 2016 July 01.

Published in final edited form as:

Dev Neurobiol. 2015 July ; 75(7): 757–777. doi:10.1002/dneu.22246.

The Dynein Inhibitor Ciliobrevin D Inhibits the Bi-directional Transport of Organelles along Sensory Axons and Impairs NGF-Mediated Regulation of Growth Cones and Axon Branches

Rajiv Sainath and **Gianluca Gallo***

Shriners Hospitals Pediatric Research Center Department of Anatomy and Cell Biology Temple University School of Medicine 3500 N Broad St, Philadelphia PA 19140

Abstract

The axonal transport of organelles is critical for the development, maintenance and survival of neurons, and its dysfunction has been implicated in several neurodegenerative diseases. Retrograde axon transport is mediated by the motor protein dynein. In this study, using embryonic chicken dorsal root ganglion neurons, we investigate the effects of Ciliobrevin D, a pharmacological dynein inhibitor, on the transport of axonal organelles, axon extension, nerve growth factor (NGF)-induced branching and growth cone expansion, and axon thinning in response to actin filament depolymerization. Live imaging of mitochondria, lysosomes and Golgi-derived vesicles in axons revealed that both the retrograde and anterograde transport of these organelles was inhibited by treatment with Ciliobrevin D. Treatment with Ciliobrevin D reversibly inhibits axon extension and transport, with effects detectable within the first 20 minutes of treatment. NGF induces growth cone expansion, axonal filopodia formation and branching. Ciliobrevin D prevented NGF-induced formation of axonal filopodia and branching but not growth cone expansion. Finally, we report that the retrograde reorganization of the axonal cytoplasm which occurs upon actin filament depolymerization is inhibited by treatment with Ciliobrevin D, indicating a role for microtubule based transport in this process, as well as Ciliobrevin D accelerating Wallerian degeneration. This study identifies Ciliobrevin D as an inhibitor of the bi-directional transport of multiple axonal organelles, indicating this drug may be a valuable tool for both the study of dynein function and a first pass analysis of the role of axonal transport.

Keywords

Ciliobrevin D; axon transport; axon growth; axon branching; dynein; kinesin; mitochondria; lysosome; Golgi derived vesicles; latrunculin; Wallerian degeneration; tubulin tyrosination; tubulin acetylation; p150glued dynactin

Introduction

Microtubule based axonal transport is critical for the development, maintenance and survival of neurons. During development, the axonal transport of Golgi-derived vesicles, synaptic

*Corresponding author Phone: 215-926-9362 gianluca.gallo@temple.edu.

vesicles, mRNA granules, mitochondria and other organelles is considered necessary for appropriate axon extension, guidance and branching (Hollenbeck and Saxton, 2005; Colin et al., 2008; Ha et al., 2008; Jung et al., 2012; Greif et al., 2013; Spillane et al., 2013). Dysfunction of the molecular motors which transport these cargoes has been implicated in several neurodegenerative diseases such as amyotrophic lateral sclerosis (ALS), Alzheimer's disease and Huntington's Disease (Sasaki and Iwata, 1996; Williamson and Cleveland, 1999; Gunawardena et al., 2003; Pigino et al., 2003; Trushina et al., 2004; Stokin et al., 2005). Microtubule based axonal transport is driven by the motor proteins of the kinesin family and cytoplasmic dynein, hereafter referred to as kinesin and dynein, whereas actin based intracellular transport is driven by myosin family members (Hirokawa, 1998; Karki and Holzbaur, 1999; Vale, 2003). In axons, microtubules have a polarized organization with the plus ends pointing distally towards the growth cone (Baas et al., 1989). Kinesins are plus end-directed motors and dynein (DYNC1) is a minus end-directed motor (Gennerich and Vale, 2009). The polarity of axonal microtubules, in conjunction with the intrinsic microtubule end specific direction of kinesin and dynein movement, underlies the ability of neurons to bi-directionally transport organelles and other cargoes.

siRNA knockdown of dynein heavy chain (DYNC1H1) reduces axon length *in vitro* (Ahmad et al., 2006), indicating that the dynein motor complex is required for axon extension. Similarly, loss of the dynein cofactor dynactin by local ablation in the growth cone through chromophore-assisted laser inactivation (CALI), decreases growth cone advance (Abe et al., 2008). Dynein may directly contribute to axon extension by regulating the transport of short microtubules in axons, by regulating the extension of microtubules into the growth cone periphery or by regulating microtubule plus ends (Myers and Baas, 2007; Liu et al., 2010; Lin et al., 2011; Nadar et al., 2012; Lazarus et al., 2013). Less is known about the involvement of dynein in axon branching. However, *Drosophila* dynein light chain mutants exhibit defects in sensory axon terminal arborization, with branches occurring aberrantly or not at all (Murphey et al., 1999).

Ciliobrevin D was discovered as an inhibitor of dynein ATPase activity, preventing the cycling activity of the motor protein (Ye et al., 2001; Cao et al., 2003; Janiesch et al., 2007; Chou et al., 2011; Firestone et al., 2012). Ciliobrevin D does not impair kinesin 1 (KIF5)-dependent microtubule gliding *in vitro* or the ATPase activity of kinesin-1 and kinesin-5 (KIF11), nor does it disrupt the association between ADP-bound dynein and microtubules in a co-sedimintation assay (Firestone et al., 2012). The effects of Ciliobrevin D on dynein driven cellular transport have been confirmed in cell systems, such as the repositioning of the microtubule organizing center in T-cells, where the effects of Ciliobrevin D are comparable to that of siRNA against the dynein heavy chain and expression of a dominant-negative fragment of p150 glued, as well as inhibiting dynein dependent melanosome aggregation (Firestone et al., 2012; Yi et al., 2013).

In this study we address the effects of Ciliobrevin D on the axonal transport of mitochondria, Golgi-derived vesicles, lysosomes as well as multiple aspects of axonal biology. Ciliobrevin D inhibited the bi-directional transport of all these organelles in embryonic sensory axons *in vitro*, an effect later discussed in the context of prior demonstrations of bi-directional effects of inhibiting dynein function. Ciliobrevin D

treatment impairs axon extension and NGF-induced axon branching. Ciliobrevin D also inhibits the retrograde redistribution of axonal cytoplasm that occurs in response to acute actin filament depolymerization but promotes Wallerian degeneration following axotomy. Collectively, these observations indicate that Ciliobrevin D may be a valuable tool for first pass analysis of hypothesis involving a role for axonal transport, minimally of the transport of the set of organelles investigated in this study, and dynein in primary neurons.

Methods

Cell Culture and Transfection

Fertilized chicken eggs containing embryos of either sex were obtained from Charles River. Embryonic day 7 chicken dorsal root ganglion neurons were cultured either as dissociated cells, for experiments involving electroporation or dye labeling, or explants. All culturing was performed on laminin-coated substrata (25 μg/ml; Invitrogen) in defined F12H (Invitrogen) serum-free medium with supplements as previously described in and detailed in (Lelkes P.I., 2006). NGF (R&D Systems) was used at 20 ng/ml except for the experiments in Figure 3 and 4 which used 40 ng/ml. Explants and dissociated cell cultures were used for experiments between 20 and 30 h after plating. For live imaging experiments, explants or dissociated cells were plated in glass-bottom dishes as described in (Ketschek and Gallo, 2010).

Dissociated DRG cells were transfected using an Amaxa Nucleoporator (program G-13, 10 μg of plasmid) and chicken transfection reagents, as previously described by (Ketschek and Gallo, 2010). For experiments in which the cultures were fixed, cells or explants were cultured on glass coverslips.

Constructs, Drugs and Organelle Stains

The NPYss-mCherry plasmid was a kind gift from Dr. G. Banker (Oregon Health and Science University) and adapted from the NPYss-GFP previously described (El Meskini et al., 2001). The drugs latrunculin A (Molecular Probes) and Ciliobrevin D (EMD Chemicals), both in DMSO, and the dyes MitoTracker Green and LysoTracker Red, both from Invitogen, were prepared according to manufactures' directions and stocks were stored at −20°C at concentrations 1000-fold greater than those used in experiments. We observed that following reconstitution, after 1 week at 4° or 3 months at −20°, the drug lost efficacy based on its effects on axon extension and growth cone morphology. Thus, it is recommended that freshly reconstituted Ciliobrevin D be used for experimentation. MitoTracker Green was used at 25 nM and LysoTracker Red was used at and 75 nM. Live cells were labeled with the dyes for 30 min in culturing medium, followed by three washes of medium prior to imaging.

Imaging

Phase and wide-field epifluorescence imaging of live (dissociated or ganglion explants) or fixed cells was performed on Zeiss Axiovert inverted microscopes equipped with a heated stage for live-cell imaging (Ketschek and Gallo, 2010). For all live-cell imaging, cultures are

allowed to equilibrate for 15 min on the heated stage prior to imaging. An Orca ER camera (Hamamatsu) was used for all wide-field image acquisition.

Immunocytochemistry

Cultures were fixed using 0.25% glutaraldehyde (Figure 2A, B, C) or cultures were simultaneously fixed (0.25% glutaraldehyde) and extracted (0.1% TX-100) in cytoskeletal buffer to only reveal polymeric cytoskeletal components (Figure 3 and 4), as previously described (Gallo and Letourneau, 1998). Glutaraldehyde fluorescence was quenched with 2 mg/ml sodium borohydride in calcium magnesium-free PBS for 15 min. Samples were then blocked using 10% goat serum in PBS with 0.1% Triton X-100 (GST) and stained with primary antibodies for 45 min, washed in GST, washed in deionized water, and mounted in no-fade mounting medium (As described by Gallo and Letourneau, 1999). Tubulin was detected using anti–α-tubulin (DM1A- FITC 1:100; Sigma) and actin filaments using rhodamine-phalloidin (1:20; Invitrogen). Tyrosinated and acetylated tubulin levels were investigated using previously described immunocytochemical and analytical protocols and reagents (Jones et al., 2006; Ketschek et al., 2007). Endogenous p150Glued dynactin was detected using the immunological reagents and protocols described in Grabham et al. (2007).

Analysis of axon branching and kymography

Branches were defined as described in (Spillane et al., 2012). Briefly, mature collateral branches along the axon shaft are defined as an axonal protrusion >10μm in length that contained one or more microtubules and exhibited secondary branches or a distal polarized distribution of actin filaments. Axonal filopodia were defined as F-actin-based protrusions that did not exhibit additional protrusive structures at their tip and a polarized distribution of filaments. Kymograph construction and analysis was performed using the MultipleKymograph plugin for NIH ImageJ and analyzed using ImageJ.

Analysis of axon degeneration following severing

The extent of varicosity formation along axons was determined using the Image J particle analysis algorithm. In phase contrast images varicosities appear as enlarged segments of the axon which are more phase dark than the rest of the axon. Images were thresholded so that only varicosities remained in the image and the percentage of area of the image representative of varicosities was determined. The total area covered by axons was similarly determined using a lower threshold and not found to differ between the images at any time points and between treatment groups (ANOVA, $p=0.94$).

Statistical Analysis

All data sets were analyzed using Instat 3 software (GraphPad Inc.). The software automatically tests the normalcy of the data sets through the Kolmogorov-Smirnov test. If any data set in an experimental design was not normal then non-parametric analysis was performed (Mann-Whitney). Parametric data sets are presented as means and standard error of measurements, nonparametric data sets are presented as distributions of data points. If all sets were normally distributed then Welch t-tests were used. Data sets binned into categories

were analyzed through the Chi-squared test using the raw categorical data, and data are presented as percentages in graphs.

Results

Ciliobrevin D inhibits both the retrograde and anterograde transport of organelles and vesicles

We first determined the effects of Ciliobrevin D on the axonal transport of mitochondria, lysosomes and Golgi-derived vesicles. For these initial experiments we utilized 20 μM Ciliobrevin D, a dose reported to maximally affect dynein based transport mechanisms in previous studies (Engel et al., 2011; Firestone et al., 2012). To directly observe the effect of Ciliobrevin D treatment on the motility of mitochondria, we performed time lapse analysis of mitochondria labeled with MitoTracker Green dye. Mitochondria were labeled by incubating dissociated sensory neuron cultures in MitoTracker Green (25 nM) for 45 minutes while being also treated with 20 μM Ciliobrevin D or DMSO, as a vehicle control, and then observing the dynamics of mitochondria in three second intervals for 120 frames. In control cultures 40.8% of mitochondria moved at least 2 μm in a single bout within the timeframe analyzed, and are referred to as motile mitochondria. Motile mitochondria spent on average 21.3 ±4% of time moving anterograde, 13.8±2% of time moving retrograde and 67.5±% of time stalled (Fig. 1A,G, Courchet et al., 2013). Interestingly, while treatment with Ciliobrevin D prevented the retrograde movement of mitochondria, anterograde movement was also impaired. The number of motile mitochondria was reduced to 13.6%, compared to 40.8% in controls. In the motile population, mitochondria spent on average 7.1 ±2% of time moving anterograde, 7.4±3% of time moving retrograde and 85.4±2% of time stalled (Fig. 1B,G; $p<0.001$ compared to control). Thus, even the mitochondria that underwent some motility in the presence of Ciliobrevin D exhibited decreased engagement of both retrograde and anterograde transport.

To determine the effects of Ciliobrevin D on the transport of additional intracellular cargoes, we performed time-lapse analysis of lysosome movement. Using the same experimental paradigm we used for imaging mitochondria, we determined that 44.3% of control LysoTracker Red labeled lysosomes are motile (Fig. 1C, G). Similar to mitochondria, after a 45 minute incubation in Ciliobrevin D, the percentage of motile lysosomes was reduced to 0.7% (Fig. 1D,G; $p<0.001$). To further analyze the effects of Ciliobrevin D treatment on the transport of membranous cargoes in axons, we expressed the NPYss-mCherry plasmid in dissociated sensory neurons. This results in the expression of mCherry targeted to Golgi-derived vesicles by the preproneuropeptide Y precursor signal (El Meskini et al., 2001). In DMSO control cultures 84.4% of mCherry-labeled vesicles are motile (Fig. 1E.G). Ciliobrevin D reduced the percentage of motile vesicles to 17.9% (Fig. 2F,G; $p<0.001$). These data reveal that although Ciliobrevin D acts directly on dynein and does not affect kinesins 5 and 1 in cell free assays (Firestone et al., 2012), in cultured embryonic sensory axons, Ciliobrevin D affects not only the retrograde movements of membranous cargoes, but also their anterograde movements, resulting in stalling of these transport cargoes.

Ciliobrevin D treatment results in a redistribution of p150Glued dynactin

The dynactin complex regulates multiple aspects of dynein function and the p150Glued subunit of the complex is crucial for this regulation (Vallee et al., 2012). We used an established immunocytochemical protocol to image the distribution of endogenous p150 dynactin in axons and growth cones (Grabham et al., 2007; n=66 and 71 axons for DMSO and Ciliobrevin D treated axons sampled from a total of 6 cultures). In 56% of axons treated with DMSO p150 dynactin exhibited either a diffuse distribution or a diffuse distribution with small puncta (Figure 1H). In the remaining 44% of axons, p150 dynactin also labeled linear profiles (Figure 1I), likely reflective of mitochondria based on their morphology and lengths. In contrast, 87% of Ciliobrevin treated axons exhibited multiple p150 dynactin labeled linear profiles, and the staining intensity of these profiles was greater than in DMSO treated axons (Figure 1H,I). Counts of the number of p150 dynactin stained linear profiles in the distal 50 μm of axons revealed median values of 2 and 6 for DMSO and Ciliobrevin D treatments, respectively ($p<0.0001$). This effect of Ciliobrevin D was also evident considering only axons that exhibited one or more profiles (medians of 3 and 7, $p<0.0001$). Analysis of the mean intensity of p150 dynactin staining in regions of interest defined by linear profiles in the distal 50 μm of axons yielded a 21% increase in the Ciliobrevin D treated axons ($p<0.0001$; n=161 and 293). In both DMSO and Ciliobrevin D treated axon populations, the distribution of cytoplasmic p150 dynactin staining in axons exhibiting linear profiles was similarly distributed amongst a diffuse or punctate background. Considering only axons exhibiting linear profiles, 59% and 62% of axons exhibited a diffuse pattern of p150 dynactin staining in DMSO and Ciliobrevin D treated groups. Similarly, considering all axons, regardless of the presence of detectable linear profiles, 34% and 35% of axons in DMSO and Ciliobrevin D treatment exhibited a diffuse p150 dynactin staining pattern in the cytoplasm, indicating Ciliobrevin D does not affect the relative distributions of axons exhibiting these two types of p150 dynactin distribution. However, although not readily quantifiable, in approximately 50% of the Ciliobrevin D treated axons classified as exhibiting a punctate distribution the puncta appeared brighter and on a background of lower cytoplasmic intensity than that evident in the DMSO treated axons (compared the representative examples in Figure 1H, punctate DMSO vs punctate Ciliobrevin D). Although Ciliobrevin D treatment caused a redistribution of p150 dynactin staining in axons, Ciliobrevin D did not affect the net staining intensity for p150 dynactin in the distal 50 μm of axons ($p>0.6$). These observations indicate that Ciliobrevin D results in the accumulation of p150 dynactin on linear structures, likely reflective of mitochondria, and smaller puncta possibly reflective of vesicles.

Ciliobrevin D reversibly inhibits axon extension

Analysis of the effects of chronic (24 hr) treatment with Ciliobrevin D concentrations between 5-40 μM applied at the time of culturing on the extension of axons from sensory explants cultured in the presence of NGF showed that concentrations greater than 5 μM resulted in a strong inhibition of axon extension and that treatment with 10 μM completely blocked axon extension (not shown). To quantify axon extension, cultures were fixed and stained with anti α-tubulin to visualize axons (Fig. 2A,B). 5 μM chronic Ciliobrevin D treatment decreased the extension of axons by approximately 50% relative to the DMSO controls (Fig. 2A,B,C). Axons from control explants extend on average 502±28μm (n=46)

from the explant, in contrast to Cilobrevin D treated explants which extend axons on average 261±17μm in length (Fig. 2C n=46, $p<0.001$).

We next investigated the time course of the effects of acute Ciliobrevin D treatment on the rate of axon extension. Sensory explants cultured overnight in NGF were treated with either DMSO control (Fig. 2D, n=60) or 20 μM Ciliobrevin D (Fig. 2E, n=59) and their net axon extension was measured over a period of 90 minutes following treatment. Acute Ciliobrevin D treatment reduced the rate of axon extension within 20 minutes of treatment, and by 90 minutes Ciliobrevin D treated axons extended on average only 3.5±2 μm, compared to control axons which extended on average 31±4 μm (Fig. 2F).

Ciliobrevin D reversibly disrupts the pre-formed spindles of metaphase-arrested cells and melanosome aggregation (Firestone et al., 2012). To determine if Ciliobrevin D reversibly inhibits axonal outgrowth, dissociated DRG cultures were incubated in 20 μM Ciliobrevin D for 60 minutes, washed three times with either 20 μM Ciliobrevin D or DMSO containing medium and then imaged for 60 minutes. Axons where Ciliobrevin D had been washed out extended faster by 20 minutes ($p<0.05$), and by 60 minutes extended 25±6 μm, as compared to axons remaining in Ciliobrevin D, which exhibited a net axon extension of 1.4±2 μm (Fig. 2G). Note that following washout, the rate of axon extension at 60 min in Fig. 2G is similar to that of the DMSO controls at 60 min in Fig. 2F, indicating full restoration of axon extension rate. These data demonstrate that Ciliobrevin D reversibly inhibits axon extension, with rates of extension returning to control levels by 20 minutes.

Because Ciliobrevin D significantly inhibits axon extension after 20 minutes we investigated whether there was a corresponding loss of mitochondrial motility at this time, similar to that observed after longer Ciliobrevin D incubation. DRG explants were incubated in MitoTracker green for 30 minutes, followed by incubation in DMSO control media or 20μM Ciliobrevin D for 20 minutes at which point mitochondrial movement was imaged in three second intervals for 120 frames (Fig. 2H,I). After a 20 minute incubation in Ciliobrevin D, the percentage of motile mitochondria was reduced from 46.2% to 17.04%, indicating that at the time when Ciliobrevin D inhibits axonal extension there is a corresponding reduction in mitochondrial motility (Fig 2J, $p<0.0001$).

Ciliobrevin D inhibits the NGF induced formation of axonal filopodia and branches but not the NGF induced increase in growth cone area.

NGF drives several functions critical to the development of axons, including axon extension and branching. Two major effects of NGF on sensory neurons are to increase the size of the growth cone and induce the formation of axonal filopodia and branches (Letourneau, 1978; Gundersen and Barrett, 1979; Paves and Saarma, 1997; Gallo and Letourneau, 1998; Ketschek and Gallo, 2010; Spillane et al., 2012). To determine the effects of Ciliobrevin D on NGF induced growth cone expansion, E7 sensory explants were cultured overnight in the absence of NGF and then treated for 40 min with or without NGF (40 ng/mL; Fig. 3A,B) and/or 20 μM Ciliobrevin D (Fig. 3C,D). Following treatments, cultures were simultaneously fixed and extracted to remove soluble tubulin and actin while preserving microtubules and actin filaments to view the cytoskeleton (Gallo and Letourneau, 1999). NGF induced a nearly threefold increase in the area of growth cones from 25±3.4μm^2 in

DMSO control treated cultures to 79±9.2 μm^2 (Fig. 3E). Treatment with Ciliobrevin D did not change the average growth cone area 32±3.1 in the absence of NGF treatment (Fig. 3E). Similarly, Ciliobrevin D did not prevent the NGF induced expansion of the growth cone (Fig. 3E). NGF treatment increased the median number of filopodia at growth cones from 1 to 5 (Fig. 3F). While, Ciliobrevin D did not affect NGF induced growth cone expansion, it reduced the number of NGF induced growth cone filopodia from a median of 5 to 2.5 (Fig. 3F). In the absence of NGF treatment Ciliobrevin D treatment alone also increased the number of growth cone filopodia, from a median of 1 to 2. Consistent with prior studies involving dynein depletion, Ciliobrevin D treated growth cones contained microtubules that often formed loops and were confined to the central domain in both no NGF and NGF treatment conditions (Myers et al., 2006).

The first step in the formation of a collateral axon branch is the formation of an axonal filopodium. Axonal filopodia emerge from actin based precursor structures termed “actin patches” (Gallo, 2006; Loudon et al., 2006). To determine the effects of Ciliobrevin D on NGF induced filopodia formation and branching, E7 sensory explants were cultured overnight in the absence of NGF and then treated for 40 min with or without NGF (40 ng/mL; Fig. 4A,B) and/or 20 μM Ciliobrevin D (Fig. 4C,D). A 40 minute treatment with NGF increased the number of filopodia in the distal 100μm of the axon (Fig. 4E). While Ciliobrevin D did not change the number of filopodia when compared to DMSO control cultures not treated with NGF, Ciliobrevin D impaired the NGF-induced increase in the number of axonal filopodia (Fig. 4E).

The second step in the formation of an axon branch is the extension and stabilization of microtubules in filopodia (Reviewed in Gallo, 2011). At the sites of nascent branches, microtubules undergo localized reorganization and fragmentation into smaller microtubules, which may target microtubules into filopodia through motor-protein driven transport (Yu et al., 1994; Baas et al., 2006). NGF promotes axon branching through both increasing the formation of axonal filopodia and the targeting of microtubules into filopodia (Ketschek and Gallo, 2010; Spillane et al., 2011; Spillane et al., 2012; Spillane et al., 2013). Thus we investigated whether Ciliobrevin D alters the percentage of filopodia that contain microtubules (Gallo and Letourneau, 1999). As expected, treating cultures with NGF for 40 minutes increased the percentage of filopodia that contained microtubules from 30.8% to 43.8%. Treating cultures with Ciliobrevin D in the absence of NGF did not affect the targeting of microtubules into filopodia (23.9% compared to 30.8%; Fig. 4F). In the presence of NGF, Cilobrevin D reduces the percentage of filopodia containing microtubules, 43.8% in NGF treated cultures compared to 18.6% when treated with both Ciliobrevin D and NGF (Fig. 4F, $p<0.05$). These data indicate that Ciliobrevin D sensitive mechanisms are involved in the NGF-induced targeting of microtubules into axonal filopodia.

Ciliobrevin D also affected the length of filopodia along the axon shaft. In the presence of NGF control filopodia exhibited an average length of 9.7±0.4μm compared to Ciliobrevin D incubated filopodia which had an average length of 6.9±4μm (Fig. 4G, $p< 0.0001$). A more in depth examination revealed that Ciliobrevin D inhibited the extension of filopodia that did not contain microtubules (filopodia w/actin only, Fig 4G; $p<0.001$), with control filopodia having mean lengths of 9.5±0.6μm compared to 6.7±0.5μm in the presence of Ciliobrevin D

(Fig. 4G). Interestingly, the length of filopodia that contained microtubules did not differ significantly, with an average of 10.1±0.5μm for control axons and 9.2±1.4μm in Ciliobrevin D (Fig. 4G).

As previously described in Spillane et al. (2011), mature collateral branches are defined as an axonal protrusion >10μm in length that contains one or more microtubules and exhibits secondary filopodia or lamellipodia based protrusive structures. As stated above, Ciliobrevin D treatment reduces the NGF induced formation of axonal filopodia and percentage of axonal filopodia that contain microtubules, both of which are necessary steps to form collateral axon branches, thus we also determined whether treatment with Ciliobrevin D also inhibits NGF-induced axon branching. As expected, following treatment with NGF 46% of axons exhibited 1 or more branches compared to 4.4% of axons in the absence of NGF (Fig. 4H, $p<0.001$). Ciliobrevin D treatment in the absence of NGF treatment did not affect the low level of baseline branching (3.5% vs 4.4% for Ciliobrevin D and DMSO controls, respectively). However, in the presence of Ciliobrevin D treatment with NGF failed to elicit branching (Fig. 4H, $p<0.001$). Thus, consistent with the effects of Ciliobrevin D on the NGF-induced formation of axonal filopodia and the targeting of microtubules into filopodia, Ciliobrevin D also inhibits NGF-induced axon branching.

Effects of Ciliobrevin D on tubulin post-translational modifications

Post-translational modification of tubulin can affect a variety of microtubule functions and their dynamics (Janke and Bulinski, 2011), and dynein associates with microtubule plus tip regulatory proteins and impacts microtubule dynamics (Vallee et al., 2012; Duellberg et al., 2014). We determined if Ciliobrevin D alters the levels of tyrosinated and acetylated α-tubulin, two modifications reflective of the relative stability of microtubule polymer. Cultures were simultaneously fixed and extracted to remove soluble tubulin while preserving microtubules and stained with anti-α-tubulin to reveal total microtubule polymer and anti-post-translationally modified tubulin antibodies as in our previous work (Jones et al., 2006; Ketschek et al., 2007). The absolute total levels of staining in a fixed length of distal axon (50 μm) were then determined and also considered as the ratio of post-translationally modified tubulin to total α-tubulin. Treatment with Ciliobrevin D (20 μM, 30 min) decreased the total microtubule content of distal axons (Figure 5A). Similarly, Ciliobrevin D decreased both the absolute and relative levels of tyrosinated and acetylated tubulin in distal axons relative to total microtubule polymer levels (Figure 5B-E).

Ciliobrevin D minimizes Latrunculin A induced retrograde cytoplasmic redistribution.

Axon extension requires assembly and reorganization of the cytoskeleton, which includes actin polymerization and depolymerization (Letourneau, 2009). Previous work from our lab demonstrated that in embryonic sensory explants which had previously extended axons for 24 hrs, overnight incubation with latrunculin A, which decreases F-actin by binding soluble actin rendering it polymerization incompetent (Coue et al., 1987; Spector et al., 1989), results in the thinning and retraction of axons (Jones et al., 2006). To investigate this process further, we treated sensory explants cultured in NGF overnight, which have established axons, with 5μM latrunculin A and observed the behavior of the distal 40μm of axons every three minutes over the course of one hour. Latrunculin A caused a disto-proximal thinning

of axons and a retrograde evacuation of cytoplasm from the tip of axons in 79% of axons, had no obvious effect in 17%of axons, and in 4% of axons a slight distal extension of cytoplasm was observed (Fig. 6A,B). During this acute treatment paradigm we did not observe retraction of the distal-most extent of the tip of the axon from its original position. The most pronounced effect of latrunculin A treatment was the apparent disto-proximal retrograde evacuation of cytoplasm, as also reflected by a decrease in the darkness of the axon shaft using phase-contrast imaging (Fig. 6A,C). Consistent with the notion that latruculin A induces retrograde redistribution of the cytoplasm and organelles, we found that a 20 min treatment decreased the number of MitoTracker Green labeled mitochondria targeted to the distal 20 μm of the axons by 29% ($p<0.01$; n=71 and 95 for DMSO and latrunculin A treatment, respectively). By one hour following treatment with latrunculin A only a few axons retained one or more mitochondria in their distal 40 μm segment, indicating continued evacuation of mitochondria with prolonged treatment (not shown).

Inhibition of dynein and interactions between microtubule and actin filament based motor proteins have been suggested to induce some forms of axon retraction and reorganization, providing a rationale for testing whether Ciliobrevin D may alter the response of axons to actin filament depolymerization (Baas and Ahmad, 2001). We thus investigated whether the latrunculin A induced redistribution of cytoplasm and axon thinning from the distal tips of axons is affected by treatment with Ciliobrevin D. Addition of Ciliobrevin D reduced the cytoplasmic redistribution caused by latrunculin A, reducing the percentage of axons that exhibited axon thinning to 26%, raising the percent of axons that undergo no change to 42% and increasing the axons that undergo extension to 42% (Fig. 6A,B, $p<0.0001$).

To quantify the amount of axon thinning we measured the total area of distal 40μm of the axon over the course of 60 minutes (Fig. 6C). In the presence of 5μm latrunculin A, the area of the axons undergoes a 48% reduction from 62.7±4.9 μm^2 to 32.5±3.5 μm^2 after 60 minutes, indicative of the extent of cytoplasmic withdrawal (Fig. 6C,D, $p<0.0001$). Cotreatment with Ciliobrevin D reduced this latrunculin A dependent change in distal axon area to 17%, with axon area changing from 66.5±4.2 μm^2 to 55.2±2.6 μm^2 after 60 minutes (Fig. 6C,D, $p<0.0001$).

Ciliobrevin D accelerates Wallerian degeneration and impairs the response of the axonal actin cytoskeleton to severing

Following severing, the distal segments of axons undergo Wallerian degeneration (Conforti et al., 2014; Freeman, 2014), and malfunction of dynein has been implicated in age/disease dependent and excitotoxic axonal degeneration (LaMonte et al., 2002; El-Kadi et al., 2007; Fujiwara et al., 2012; Ikenaka et al., 2012). To test whether dynein may also be involved in the mechanism of Wallerian degeneration we severed axons growing from explants at the base of the explant (Figure 7A) and tracked their degeneration over time. To provide sufficient lengths of axons the explants were cultured for 48 hrs. The formation of varicosities/beads is a hallmark of axon degeneration. Treatment with 20 μM Ciliobrevin D at the time of axotomy promoted the formation of varicosities along axons relative to control DMSO treated cultures at 3 and 5 hrs following axon severing (Figure 7B,C). At the 5 hr time point, cultures were simultaneously fixed and extracted and stained to reveal

microtubules and actin filaments. In DMSO treated cultures, the axons on the severed side of the explant exhibited increases in actin filaments levels, often distributed uniformly throughout the shaft of the axon (Figure 8A,B). In contrast, Ciliobrevin D treated severed axons did not exhibit uniformly distributed actin filaments but rather exhibited local accumulations of filaments along the axon shaft (Figure 8A,B). These data indicate that dynein activity counters severing-induced axon degeneration and that it contributes to severing-induced reorganization of actin filaments in severed axons, which may have a protective function in the context of Wallerian degeneration.

Discussion

The active transport of cargoes along the axon is critical for the development, maintenance and regeneration of axons (Prokop, 2013). The anterograde transport of proteins, vesicles, organelles and mRNA is necessary for proper axon growth and guidance as well as the targeted formation of axon branching (Hollenbeck and Saxton, 2005; Ha et al., 2008; Jung et al., 2012; Spillane et al., 2013). Dynein mediated retrograde transport is considered to play an important role in retrograde signaling mechanisms along axons and the clearance of damaged cellular components (Hirokawa et al., 2010). However, inhibition of dynein function also impacts the forward extension of axons, which is otherwise considered to rely on anterograde transport mechanisms, as reflected by studies demonstrating that dynein knockdown in DRG cultures inhibits axon outgrowth (Ahmad et al., 2006; Grabham et al., 2007). Furthermore, dynein light chain *drosophila* knockout mutants, display reduced density of axon tracts, mistargeting of axons, and defects in branching *in vivo*, indicating that dynein function is necessary for the development of axons (Phillis et al., 1996; Murphey et al., 1999). It should be noted that overexpression of p50-dynamitin, which inhibits dynein function, or a rigorous protocol of dynein heavy chain knockdown also causes axons to develop misaligned microtubules within axons (Echeverri et al., 1996; Ahmad et al., 2006). Similar to the effects of dynein knockdown, we report that chronic treatment with the dynein inhibitor Ciliobrevin D reduces axon extension. The effect of Ciliobrevin D on axon extension is evident within 20 minutes of treatment of previously established axons, indicating that active transport is required for active axon elongation. Importantly, after washing out Ciliobrevin D, axon extension returns to control levels within ten minutes, enabling manipulation of dynein activity within a short temporal window. These observations using Ciliobrevin D to inhibit dynein function further indicate that the dynamic regulation of dynein activity in axons contributes to axon extension.

Ciliobrevin D is an inhibitor of the dynein ATPase, which is required for its motor protein activity (Firestone et al., 2012). Ciliobrevin D inhibits the activity of dynein but not kinesin 1 or 5 in *in vitro* reconstituted motor protein assays (Firestone et al., 2012). Our study reveals that treatment of cultured embryonic sensory neurons with Ciliobrevin D blocks, as expected, the retrograde transport of organelles (mitochondria, lysosomes and Golgi-derived vesicles), but also their anterograde transport. Thus, Ciliobrevin D acts as an inhibitor of the bidirectional axonal transport of these organelles. The bidirectional effect of inhibiting dynein activity or depleting dynein has precedent. In *Drosophila* S2 cells, dynein knockdown prevents all peroxisome transport, not just unidirectional transport (Ally et al., 2009). These effects can be rescued by replacing the lost motor protein with an unrelated,

peroxisome motor of the same directionality. Similarly, Kim et al. (2007) also observed a bidirectional block of peroxisome motility in *Drosophila* cells following dynein depletion. In axons, cytoplasmic dynein and kinesin mutants display genetic interactions with respect to defects in cargo localization, suggesting they are interdependent for fast axonal transport (Martin et al., 1999). Similarly, Fejtova et al. (2009) found that interfering with the binding between dynein light chains and the synaptic vesicle protein bassoon impaired both retrograde and anterograde movements of synaptic vesicles. Furthermore, injection of dynein function blocking antibodies or treatment with Ciliobrevin D also bidirectionally affected bulk cytoskeletal movements in axons, and injection of function blocking antibodies caused stalling of lysosomes in COS-7 cells (Yi et al., 2011; Roossien et al., 2014). The anterograde transport of neurofilaments was also found to be impaired by inhibition of dynein function through multiple approaches (Uchida et al., 2009). A concern with studies addressing dynein light chains (e.g., LC8/DYNLL) is that these proteins may have roles outside of dynein (Rapali et al., 2011). The observations from the current study using Ciliobrevin D indicate that impairment of dynein ATPase activity alone can account for its role in the regulation of both retrograde and anterograde transport, although undiscovered effects of Ciliobrevin D on dynein structure cannot currently be ruled out.

This study revealed that treatment with Ciliobrevin D inhibits both retrograde and anterograde fast axonal transport. Axonal mitochondria move by fast axonal transport which is to varying degrees saltatory and bidirectional (Reviewed in Hollenbeck and Saxton, 2005). Likewise, lysosomal and Golgi derived vesicular transport occurs via fast axonal transport both anterogradely and retrogradely, all of which was inhibited by Ciliobrevin D (Hirokawa and Takemura, 2005). These data indicate that Ciliobrevin D can be used as a tool to inhibit the fast axonal transport of the classes of membranous organelles investigated in this report. Additional studies will be required to screen additional cargoes. The anterograde transport of mitochondria is mediated by kinesin 1 (KIF5) and the retrograde transport by dynein (Schwarz, 2013). The anterograde transport of lysosomes can be mediated by the KIF5, KIF3A/3B, KIF1Bβ and KIF2β kinesins and retrograde transport is mediated by dynein (Hirokawa and Noda, 2008; Granger et al., 2014) The anterograde and retrograde transport of Golgi derived synaptic vesicles is dependent on KIF1A and KIF5B and dynein, respectively (Okada et al., 1995; Yonekawa et al., 1998; Cai et al., 2007; Fejtova et al., 2009). Thus, it would be predicted that additional axonal cargoes using these combinations of anterograde kinesins and retrograde dynein motor proteins may be similarly affected by Ciliobrevin D. Furthermore, recent evidence indicates that the mechanism of slow axonal transport, which conveys non-membranous cargoes, relies on the same motor systems and mechanism as fast axonal transport (Scott et al., 2011; Tang et al., 2013). It will be of interest to test whether Ciliobrevin D also affects slow axonal transport (Roy, 2014).

The targeting of dynein to transport cargoes, or subcellular domains (e.g., the nuclear envelope), is an important aspect of the regulation of dynein function (Vallee et al., 2012). Dynactin is involved in the recruitment of dynein to some, but not all, cargoes (Haghnia et al., 2007; Tan et al., 2011; Vallee et al., 2012). The observation that Ciliobrevin D treatment induced a redistribution of p150 dynactin within axons also indicates that the ATPase activity of dynein may be involved either in the targeting or retention of the dynein-dynactin

complex on axonal organelles. It will be of interest to further investigate the role of dynein ATPase function in the targeting of dynein and dynactin to cargoes and organelles.

Based on the observation that Ciliobrevin D acts as a bidirectional inhibitor of the axonal transport of mitochondria, lysosomes and Golgi derived vesicles, we sought to determine its utility as a reagent for addressing the role of dynein-dependent axonal transport in biological phenomena. To this end, we used NGF-induced branching, as this is a mechanism which is considered to rely on aspects of axonal transport, which have however only been minimally explored. For example, the delivery of synaptotagmin 1 containing vesicles promotes the formation of axonal filopodia and branches (Greif et al., 2013), depletion of the kinesin adaptor calsyntenin-1 impairs branching (Ponomareva et al., 2014) and mitochondrial localization has recently been shown to have an important role in axon branching (Courchet et al., 2013; Greif et al., 2013; Spillane et al., 2013; Tao et al., 2014). The effects of Ciliobrevin D indicate that dynein-dependent transport based mechanisms contribute to the formation of NGF-induced axonal filopodia, and the ability of microtubules to enter or be retained in axonal filopodia. Consistent with prior studies on dynein function, Ciliobrevin D also caused the looping of microtubules in growth cones and inhibited the targeting of microtubules into filopodia (Ahmad et al., 2006). The effects of Ciliobrevin D on microtubules, reflective of dynein inhibition, indicate that dynein activity is required for the second step in collateral branch formation, the invasion of axonal filopodia by microtubules. Interestingly, although filopodia along Ciliobrevin D treated axons were shorter in length, the few that contained microtubules exhibited similar lengths as control filopodia. This observation indicates that once a microtubule is targeted into an axonal filopodia, it regulates its length independent of dynein activity. Indeed, microtubule tips exhibit a variety of possible signaling functions due to the cohort of associated proteins (Dent and Baas, 2014). Consistent with previously discussed studies reporting a role for dynein in axon extension, Ciliobrevin D also impaired the extension of the main axon. The effects of Ciliobrevin on axon extension are not unexpected given its general inhibition of the bidirectional transport of mitochondria and Golgi derived vesicles, both of which contribute to axon extension (Jareb and Banker, 1997; Steketee et al., 2012; Spillane et al., 2013), and its effects on microtubules in distal axons. Interestingly, the NGF-induced expansion of the growth cone was not found to be affected by Ciliobrevin D. This may reflect the pre-existing positioning of relevant organelles at the growth cone which are not required to undergo transport in order to have roles in the regulation of growth cone expansion.

Ciliobrevin D exhibited complex effects on growth cone filopodia. In the absence of NGF, Ciliobrevin D treatment increased the number of filopodia. However, Ciliobrevin D largely inhibited the NGF-induced increase in the number of growth cone filopodia as NGF treatment only slightly increased the number of filopodia above the levels present in the presence of Ciliobrevin D alone. At present the mechanistic basis for these effects is unclear, but indicate that dynein or organelle motility may have non-conserved roles in the regulation of growth cone filopodia as a function of NGF treatment on laminin substrata. We have seen a similar NGF-dependent effect of the myosin II inhibitor blebbistatin on growth cone protrusive dynamics in other ongoing studies (not shown), indicating that NGF may alter the mechanisms underlying growth cone protrusive activity relative to those activated by laminin signaling alone. A component of the mechanism that may underlie the differences in

filopodia in the presence of NGF relative to the absence of NGF on laminin is the myosin motor-dependent NGF-induced redistribution of integrin receptors to filopodia (Grabham and Goldberg, 1997; Grabham et al., 2000). Dynein can exhibit interplay with myosin family members (e.g., myosin II; Myers et al., 2006) and is recruited to the leading edge of growth cones by laminin (Grabham et al., 2007), the data may reflect this type of interaction in an NGF regulated manner, but will require future analysis.

Ciliobrevin D treatment resulted in an approximately 30% decrease in the total levels of microtubule polymer in distal axons. This finding is consistent with the emerging role of dynein and dynactin in regulating aspects of microtubule plus end dynamics, and suggest an impairment of polymerization or promotion of depolymerization. p150 dynactin has been reported to act as an anti-catastrophe factor during axonal microtubule polymerization (Lazarus et al., 2013). This observation suggests that the subcellular redistribution of p150 induced by Ciliobrevin D may be linked to the decrease in axonal microtubule mass through the promotion of catastrophes. At the time of polymerization, tubulin is in tyrosinated form and subsequently undergoes detyrosination in a time dependent manner following incorporation into microtubules (reviewed in MacRae, 1997; Janke and Bulinski, 2011). Ciliobrevin D treatment decreased the levels of tyrosinated tubulin in microtubules, generally consistent with decreased microtubule dynamics and increased stability. It is also possible that Ciliobrevin D may have resulted in an increase in non-tyrosinatable tubulin, an issue that would require further analysis. However, the acetylation of tubulin is also a time-dependent modification of tubulin in polymeric form and the levels of acetylated tubulin were also decreased by Ciliobrevin D treatment. If microtubules were less dynamic and more stable following Ciliobrevin D treatment, then the levels of acetylated tubulin would be expected to be increased by Ciliobrevin D treatment. This observation raises the possibility that dynein function/p150 distribution, or perhaps organelle motility, contributes to the dynamics of tubulin acetylation.

We previously reported that chronic depolymerization of actin filaments induces the retraction of early embryonic sensory axons (Jones et al., 2006). In the current work, we extend these observations by investigating the mechanism of this form of axon retraction/reorganization. Time-lapse imaging of the response of axons to the actin filament depolymerizing drug latrunculin A revealed a distal-proximal thinning of the axon, characterized by apparent retrograde cytoplasmic displacement. Motor protein based force generation has been suggested to underlie some forms of axon retraction (Baas and Ahmad, 2001; Ahmad et al., 2006; Hirokawa et al., 2010; Prokop, 2013). We therefore used Ciliobrevin D to address whether motor protein driven axonal transport mechanisms could contribute to actin filament depolymerization induced axon retraction. The observation that Ciliobrevin D strongly inhibited the effects of actin filament depolymerization in axons suggests that the cytoplasmic regression is driven, at least in part, by motor protein based mechanism. In contrast to axons only treated with latrunculin A, joint treatment with Ciliobrevin D increased the proportion of axons that exhibited forward elongation in the absence of actin filaments during the imaging period. This elongation is likely due to continued polymerization of microtubules in the distal axon, although this issue will require further analysis. In axons not treated with latrunculin A, Ciliobrevin D decreased the microtubule content of distal axons, and effect possibly linked to the observed redistribution

of p150 dynactin and its role as an anti-catastrophe factor (Lazarus et al., 2013). Thus, if the observed forward advance of axons is reflective of a microtubule-based mechanism, this indicates some interaction between an intact actin filament cytoskeleton and the effects of Ciliobrevin D. Generally consistent with this notion, we have previously reported that in older E14 sensory axons, which continue to exhibit some forward advance following actin filament depolymerization, the duration of microtubule plus tip polymerization events is decreased relative to E7 axons which in contrast fail to extend following filament depolymerization (Jones et al., 2006).

The mechanisms of severing-induced axon degeneration are beginning to be unveiled (Conforti et al., 2014; Freeman, 2014). The current study indicates that the actin cytoskeleton undergoes reorganization in the distal axon following severing. The reorganization of axonal actin filaments is impaired by treatment with Ciliobrevin D, indicating it is a process dependent on dynein or organelle motility. Increase in axonal actin filament levels and organization occurs in control axons during the period when degeneration is starting and may represent an intrinsic protective mechanism, which is abrogated by inhibition of dynein. Consistent with this notion, Ciliobrevin D prevented the increase in actin filaments in severed axons, accelerated the onset of varicosity formation along axons, and axon degeneration involves the caspase mediated proteolysis of actin (Sokolowski et al., 2014). It will be of interest to elucidate the mechanisms through which dynein regulates various aspects of the axonal cytoskeleton (e.g., filopodia in the context of branching and axonal actin filament reorganization/polymerization in the context of axon degeneration). In the context of severing induced axon degeneration, the RhoA pathway may be involved in the regulation the axonal actin cytoskeleton (Garland et al., 2012). Consistent with this notion, loss of the dynein regulator Lis1 results in activation of RhoA in neurons (Kholmanskikh et al., 2003). It will be of interest to determine the contribution of motor protein driven transport mechanisms in other forms of axon retraction (e.g., retraction initiated in response to axon repellents) and distal-proximal axon retraction/degeneration in response to injury or degenerative diseases (Luo and O'Leary, 2005; Gallo, 2006; Myers et al., 2006; Neukomm and Freeman, 2014).

In conclusion, we report that in chicken embryonic sensory neurons Ciliobrevin D acts as an inhibitor of the bi-directional axonal transport of mitochondria, lysosomes and Golgi-derived vesicles. As dynein is considered to be the major, if not sole, motor protein responsible for retrograde transport, Ciliobrevin D may indeed impair multiple forms of microtubule based transport through dynein-anterograde motor protein inter-dependence. This issue will require additional exhaustive investigation. It must also be considered that although the effects of Ciliobrevin D described in this work lend themselves to interpretations consistent with the literature on dynein/dynactin, off target effects of the drug cannot be ruled out. However, Ciliobrevin D may be a useful tool for a first pass test of hypothesis involving a functional role for axonal transport, which if yielding a positive result should then be followed up by more in depth molecular analysis. Finally, low doses of Ciliobrevin D may be useful to generate low to moderate degrees of impairment of axonal transport to mimic that which is considered to occur in neurodegenerative disorders.

Acknowledgements

This work was supported by an NIH award to GG (NS078030).

References

Abe TK, Honda T, Takei K, Mikoshiba K, Hoffman-Kim D, Jay DG, Kuwano R. Dynactin is essential for growth cone advance. Biochem Biophys Res Commun. 2008; 372:418–422. [PubMed: 18477476]

Ahmad FJ, He Y, Myers KA, Hasaka TP, Francis F, Black MM, Baas PW. Effects of dynactin disruption and dynein depletion on axonal microtubules. Traffic. 2006; 7:524–537. [PubMed: 16643276]

Ally S, Larson AG, Barlan K, Rice SE, Gelfand VI. Opposite-polarity motors activate one another to trigger cargo transport in live cells. J Cell Biol. 2009; 187:1071–1082. [PubMed: 20038680]

Baas PW, Ahmad FJ. Force generation by cytoskeletal motor proteins as a regulator of axonal elongation and retraction. Trends Cell Biol. 2001; 11:244–249. [PubMed: 11356360]

Baas PW, Black MM, Banker GA. Changes in microtubule polarity orientation during the development of hippocampal neurons in culture. J Cell Biol. 1989; 109:3085–3094. [PubMed: 2592416]

Baas PW, Vidya Nadar C, Myers KA. Axonal transport of microtubules: the long and short of it. Traffic. 2006; 7:490–498. [PubMed: 16643272]

Cai Q, Pan PY, Sheng ZH. Syntabulin-kinesin-1 family member 5B-mediated axonal transport contributes to activity-dependent presynaptic assembly. J Neurosci. 2007; 27:7284–7296. [PubMed: 17611281]

Cao K, Nakajima R, Meyer HH, Zheng Y. The AAA-ATPase Cdc48/p97 regulates spindle disassembly at the end of mitosis. Cell. 2003; 115:355–367. [PubMed: 14636562]

Chou TF, Brown SJ, Minond D, Nordin BE, Li K, Jones AC, Chase P, Porubsky PR, Stoltz BM, Schoenen FJ, Patricelli MP, Hodder P, Rosen H, Deshaies RJ. Reversible inhibitor of p97, DBeQ, impairs both ubiquitin-dependent and autophagic protein clearance pathways. Proc Natl Acad Sci U S A. 2011; 108:4834–4839. [PubMed: 21383145]

Colin E, Zala D, Liot G, Rangone H, Borrell-Pages M, Li XJ, Saudou F, Humbert S. Huntingtin phosphorylation acts as a molecular switch for anterograde/retrograde transport in neurons. EMBO J. 2008; 27:2124–2134. [PubMed: 18615096]

Conforti L, Gilley J, Coleman MP. Wallerian degeneration: an emerging axon death pathway linking injury and disease. Nature reviews Neuroscience. 2014; 15:394–409.

Coue M, Brenner SL, Spector I, Korn ED. Inhibition of actin polymerization by latrunculin A. FEBS Lett. 1987; 213:316–318. [PubMed: 3556584]

Courchet J, Lewis TL Jr. Lee S, Courchet V, Liou DY, Aizawa S, Polleux F. Terminal axon branching is regulated by the LKB1-NUAK1 kinase pathway via presynaptic mitochondrial capture. Cell. 2013; 153:1510–1525. [PubMed: 23791179]

Dent EW, Baas PW. Microtubules in neurons as information carriers. J Neurochem. 2014; 129:235–239. [PubMed: 24266899]

Duellberg C, Trokter M, Jha R, Sen I, Steinmetz MO, Surrey T. Reconstitution of a hierarchical +TIP interaction network controlling microtubule end tracking of dynein. Nature cell biology. 2014; 16:804–811.

Echeverri CJ, Paschal BM, Vaughan KT, Vallee RB. Molecular characterization of the 50-kD subunit of dynactin reveals function for the complex in chromosome alignment and spindle organization during mitosis. J Cell Biol. 1996; 132:617–633. [PubMed: 8647893]

El-Kadi AM, Soura V, Hafezparast M. Defective axonal transport in motor neuron disease. Journal of neuroscience research. 2007; 85:2557–2566. [PubMed: 17265455]

El Meskini R, Jin L, Marx R, Bruzzaniti A, Lee J, Emeson R, Mains R. A signal sequence is sufficient for green fluorescent protein to be routed to regulated secretory granules. Endocrinology. 2001; 142:864–873. [PubMed: 11159860]

Engel BD, Ishikawa H, Feldman JL, Wilson CW, Chuang PT, Snedecor J, Williams J, Sun Z, Marshall WF. A cell-based screen for inhibitors of flagella-driven motility in Chlamydomonas reveals a novel modulator of ciliary length and retrograde actin flow. Cytoskeleton (Hoboken). 2011; 68:188–203. [PubMed: 21360831]

Fejtova A, Davydova D, Bischof F, Lazarevic V, Altrock WD, Romorini S, Schone C, Zuschratter W, Kreutz MR, Garner CC, Ziv NE, Gundelfinger ED. Dynein light chain regulates axonal trafficking and synaptic levels of Bassoon. J Cell Biol. 2009; 185:341–355. [PubMed: 19380881]

Firestone AJ, Weinger JS, Maldonado M, Barlan K, Langston LD, O'Donnell M, Gelfand VI, Kapoor TM, Chen JK. Small-molecule inhibitors of the AAA+ ATPase motor cytoplasmic dynein. Nature. 2012; 484:125–129. [PubMed: 22425997]

Freeman MR. Signaling mechanisms regulating Wallerian degeneration. Current opinion in neurobiology. 2014; 27:224–231. [PubMed: 24907513]

Fujiwara T, Morimoto K, Kakita A, Takahashi H. Dynein and dynactin components modulate neurodegeneration induced by excitotoxicity. Journal of neurochemistry. 2012; 122:162–174. [PubMed: 22515507]

Gallo G. RhoA-kinase coordinates F-actin organization and myosin II activity during semaphorin-3A-induced axon retraction. J Cell Sci. 2006; 119:3413–3423. [PubMed: 16899819]

Gallo G. The cytoskeletal and signaling mechanisms of axon collateral branching. Dev Neurobiol. 2011; 71:201–220. [PubMed: 21308993]

Gallo G, Letourneau PC. Localized sources of neurotrophins initiate axon collateral sprouting. J Neurosci. 1998; 18:5403–5414. [PubMed: 9651222]

Gallo G, Letourneau PC. Different contributions of microtubule dynamics and transport to the growth of axons and collateral sprouts. J Neurosci. 1999; 19:3860–3873. [PubMed: 10234018]

Garland P, Broom LJ, Quraishe S, Dalton PD, Skipp P, Newman TA, Perry VH. Soluble axoplasm enriched from injured CNS axons reveals the early modulation of the actin cytoskeleton. PloS one. 2012; 7:e47552. [PubMed: 23115653]

Gennerich A, Vale RD. Walking the walk: how kinesin and dynein coordinate their steps. Curr Opin Cell Biol. 2009; 21:59–67. [PubMed: 19179063]

Grabham PW, Foley M, Umeojiako A, Goldberg DJ. Nerve growth factor stimulates coupling of beta1 integrin to distinct transport mechanisms in the filopodia of growth cones. J Cell Sci. 2000; 113(Pt 17):3003–3012. [PubMed: 10934039]

Grabham PW, Goldberg DJ. Nerve growth factor stimulates the accumulation of beta1 integrin at the tips of filopodia in the growth cones of sympathetic neurons. The Journal of neuroscience : the official journal of the Society for Neuroscience. 1997; 17:5455–5465. [PubMed: 9204928]

Grabham PW, Seale GE, Bennecib M, Goldberg DJ, Vallee RB. Cytoplasmic dynein and LIS1 are required for microtubule advance during growth cone remodeling and fast axonal outgrowth. J Neurosci. 2007; 27:5823–5834. [PubMed: 17522326]

Granger E, McNee G, Allan V, Woodman P. The role of the cytoskeleton and molecular motors in endosomal dynamics. Semin Cell Dev Biol. 2014; 31C:20–29. [PubMed: 24727350]

Greif KF, Asabere N, Lutz GJ, Gallo G. Synaptotagmin-1 promotes the formation of axonal filopodia and branches along the developing axons of forebrain neurons. Dev Neurobiol. 2013; 73:27–44. [PubMed: 22589224]

Gunawardena S, Her LS, Brusch RG, Laymon RA, Niesman IR, Gordesky-Gold B, Sintasath L, Bonini NM, Goldstein LS. Disruption of axonal transport by loss of huntingtin or expression of pathogenic polyQ proteins in Drosophila. Neuron. 2003; 40:25–40. [PubMed: 14527431]

Gundersen RW, Barrett JN. Neuronal chemotaxis: chick dorsal-root axons turn toward high concentrations of nerve growth factor. Science. 1979; 206:1079–1080. [PubMed: 493992]

Ha J, Lo KW, Myers KR, Carr TM, Humsi MK, Rasoul BA, Segal RA, Pfister KK. A neuron-specific cytoplasmic dynein isoform preferentially transports TrkB signaling endosomes. J Cell Biol. 2008; 181:1027–1039. [PubMed: 18559670]

Haghnia M, Cavalli V, Shah SB, Schimmelpfeng K, Brusch R, Yang G, Herrera C, Pilling A, Goldstein LSB. Dynactin is required for coordinated bidirectional motility, but not for dynein membrane attachment. Molecular biology of the cell. 2007; 18:2081–2089. [PubMed: 17360970]

Hirokawa N. Kinesin and dynein superfamily proteins and the mechanism of organelle transport. Science. 1998; 279:519–526. [PubMed: 9438838]

Hirokawa N, Niwa S, Tanaka Y. Molecular motors in neurons: transport mechanisms and roles in brain function, development, and disease. Neuron. 2010; 68:610–638. [PubMed: 21092854]

Hirokawa N, Noda Y. Intracellular transport and kinesin superfamily proteins, KIFs: structure, function, and dynamics. Physiol Rev. 2008; 88:1089–1118. [PubMed: 18626067]

Hirokawa N, Takemura R. Molecular motors and mechanisms of directional transport in neurons. Nat Rev Neurosci. 2005; 6:201–214. [PubMed: 15711600]

Hollenbeck PJ, Saxton WM. The axonal transport of mitochondria. J Cell Sci. 2005; 118:5411–5419. [PubMed: 16306220]

Ikenaka K, Katsuno M, Kawai K, Ishigaki S, Tanaka F, Sobue G. Disruption of axonal transport in motor neuron diseases. International journal of molecular sciences. 2012; 13:1225–1238. [PubMed: 22312314]

Janiesch PC, Kim J, Mouysset J, Barikbin R, Lochmuller H, Cassata G, Krause S, Hoppe T. The ubiquitin-selective chaperone CDC-48/p97 links myosin assembly to human myopathy. Nat Cell Biol. 2007; 9:379–390. [PubMed: 17369820]

Janke C, Bulinski JC. Post-translational regulation of the microtubule cytoskeleton: mechanisms and functions. Nature reviews Molecular cell biology. 2011; 12:773–786.

Jareb M, Banker G. Inhibition of axonal growth by brefeldin A in hippocampal neurons in culture. J Neurosci. 1997; 17:8955–8963. [PubMed: 9364043]

Jones SL, Selzer ME, Gallo G. Developmental regulation of sensory axon regeneration in the absence of growth cones. Journal of neurobiology. 2006; 66:1630–1645. [PubMed: 17058187]

Jung H, Yoon BC, Holt CE. Axonal mRNA localization and local protein synthesis in nervous system assembly, maintenance and repair. Nat Rev Neurosci. 2012; 13:308–324. [PubMed: 22498899]

Karki S, Holzbaur EL. Cytoplasmic dynein and dynactin in cell division and intracellular transport. Curr Opin Cell Biol. 1999; 11:45–53. [PubMed: 10047518]

Ketschek A, Gallo G. Nerve growth factor induces axonal filopodia through localized microdomains of phosphoinositide 3-kinase activity that drive the formation of cytoskeletal precursors to filopodia. J Neurosci. 2010; 30:12185–12197. [PubMed: 20826681]

Ketschek AR, Jones SL, Gallo G. Axon extension in the fast and slow lanes: substratum-dependent engagement of myosin II functions. Dev Neurobiol. 2007; 67:1305–1320. [PubMed: 17638383]

Kholmanskikh SS, Dobrin JS, Wynshaw-Boris A, Letourneau PC, Ross ME. Disregulated RhoGTPases and actin cytoskeleton contribute to the migration defect in Lis1-deficient neurons. The Journal of neuroscience : the official journal of the Society for Neuroscience. 2003; 23:8673–8681. [PubMed: 14507966]

Kim H, Ling SC, Rogers GC, Kural C, Selvin PR, Rogers SL, Gelfand VI. Microtubule binding by dynactin is required for microtubule organization but not cargo transport. J Cell Biol. 2007; 176:641–651. [PubMed: 17325206]

LaMonte BH, Wallace KE, Holloway BA, Shelly SS, Ascano J, Tokito M, Van Winkle T, Howland DS, Holzbaur ELF. Disruption of dynein/dynactin inhibits axonal transport in motor neurons causing late-onset progressive degeneration. Neuron. 2002; 34:715–727. [PubMed: 12062019]

Lazarus JE, Moughamian AJ, Tokito MK, Holzbaur EL. Dynactin subunit p150(Glued) is a neuron-specific anti-catastrophe factor. PLoS Biol. 2013; 11:e1001611. [PubMed: 23874158]

Lelkes, PI., UBR; Saporta, S.; Cameron, DF.; Gallo, G. Culture of neuroendocrine and neuronal cells for tissue engineering. Wiley-Liss; 2006. Chapter 14

Letourneau PC. Chemotactic response of nerve fiber elongation to nerve growth factor. Dev Biol. 1978; 66:183–196. [PubMed: 751835]

Letourneau PC. Actin in axons: stable scaffolds and dynamic filaments. Results Probl Cell Differ. 2009; 48:65–90. [PubMed: 19582412]

Lin S, Liu M, Son YJ, Timothy Himes B, Snow DM, Yu W, Baas PW. Inhibition of Kinesin-5, a microtubule-based motor protein, as a strategy for enhancing regeneration of adult axons. Traffic. 2011; 12:269–286. [PubMed: 21166743]

Liu M, Nadar VC, Kozielski F, Kozlowska M, Yu W, Baas PW. Kinesin-12, a mitotic microtubule-associated motor protein, impacts axonal growth, navigation, and branching. J Neurosci. 2010; 30:14896–14906. [PubMed: 21048148]

Loudon RP, Silver LD, Yee HF Jr. Gallo G. RhoA-kinase and myosin II are required for the maintenance of growth cone polarity and guidance by nerve growth factor. J Neurobiol. 2006; 66:847–867. [PubMed: 16673385]

Luo L, O'Leary DD. Axon retraction and degeneration in development and disease. Annu Rev Neurosci. 2005; 28:127–156. [PubMed: 16022592]

MacRae TH. Tubulin post-translational modifications--enzymes and their mechanisms of action. European journal of biochemistry / FEBS. 1997; 244:265–278. [PubMed: 9118990]

Martin M, Iyadurai SJ, Gassman A, Gindhart JG Jr. Hays TS, Saxton WM. Cytoplasmic dynein, the dynactin complex, and kinesin are interdependent and essential for fast axonal transport. Mol Biol Cell. 1999; 10:3717–3728. [PubMed: 10564267]

Murphey RK, Caruccio PC, Getzinger M, Westgate PJ, Phillis RW. Dynein-dynactin function and sensory axon growth during Drosophila metamorphosis: A role for retrograde motors. Dev Biol. 1999; 209:86–97. [PubMed: 10208745]

Myers KA, Baas PW. Kinesin-5 regulates the growth of the axon by acting as a brake on its microtubule array. J Cell Biol. 2007; 178:1081–1091. [PubMed: 17846176]

Myers KA, He Y, Hasaka TP, Baas PW. Microtubule transport in the axon: Re-thinking a potential role for the actin cytoskeleton. Neuroscientist. 2006; 12:107–118. [PubMed: 16514008]

Myers KA, Tint I, Nadar CV, He Y, Black MM, Baas PW. Antagonistic forces generated by cytoplasmic dynein and myosin-II during growth cone turning and axonal retraction. Traffic. 2006; 7:1333–1351. [PubMed: 16911591]

Nadar VC, Lin S, Baas PW. Microtubule redistribution in growth cones elicited by focal inactivation of kinesin-5. J Neurosci. 2012; 32:5783–5794. [PubMed: 22539840]

Neukomm LJ, Freeman MR. Diverse cellular and molecular modes of axon degeneration. Trends Cell Biol. 2014

Okada Y, Yamazaki H, Sekine-Aizawa Y, Hirokawa N. The neuron-specific kinesin superfamily protein KIF1A is a unique monomeric motor for anterograde axonal transport of synaptic vesicle precursors. Cell. 1995; 81:769–780. [PubMed: 7539720]

Paves H, Saarma M. Neurotrophins as in vitro growth cone guidance molecules for embryonic sensory neurons. Cell Tissue Res. 1997; 290:285–297. [PubMed: 9321690]

Phillis R, Statton D, Caruccio P, Murphey RK. Mutations in the 8 kDa dynein light chain gene disrupt sensory axon projections in the Drosophila imaginal CNS. Development. 1996; 122:2955–2963. [PubMed: 8898210]

Pigino G, Morfini G, Pelsman A, Mattson MP, Brady ST, Busciglio J. Alzheimer's presenilin 1 mutations impair kinesin-based axonal transport. J Neurosci. 2003; 23:4499–4508. [PubMed: 12805290]

Ponomareva OY, Holmen IC, Sperry AJ, Eliceiri KW, Halloran MC. Calsyntenin-1 regulates axon branching and endosomal trafficking during sensory neuron development in vivo. The Journal of neuroscience : the official journal of the Society for Neuroscience. 2014; 34:9235–9248. [PubMed: 25009257]

Prokop A. The intricate relationship between microtubules and their associated motor proteins during axon growth and maintenance. Neural Dev. 2013; 8:17. [PubMed: 24010872]

Rapali P, Szenes A, Radnai L, Bakos A, Pal G, Nyitray L. DYNLL/LC8: a light chain subunit of the dynein motor complex and beyond. The FEBS journal. 2011; 278:2980–2996. [PubMed: 21777386]

Roossien DH, Lamoureux P, Miller KE. Cytoplasmic dynein pushes the cytoskeletal meshwork forward during axonal elongation. J Cell Sci. 2014

Roy S. Seeing the unseen: the hidden world of slow axonal transport. Neuroscientist. 2014; 20:71–81. [PubMed: 23912032]

Sasaki S, Iwata M. Impairment of fast axonal transport in the proximal axons of anterior horn neurons in amyotrophic lateral sclerosis. Neurology. 1996; 47:535–540. [PubMed: 8757033]

Schwarz TL. Mitochondrial trafficking in neurons. Cold Spring Harb Perspect Biol. 2013:5.

Scott DA, Das U, Tang Y, Roy S. Mechanistic logic underlying the axonal transport of cytosolic proteins. Neuron. 2011; 70:441–454. [PubMed: 21555071]

Sokolowski JD, Gamage KK, Heffron DS, Leblanc AC, Deppmann CD, Mandell JW. Caspase-mediated cleavage of actin and tubulin is a common feature and sensitive marker of axonal degeneration in neural development and injury. Acta neuropathologica communications. 2014; 2:16. [PubMed: 24507707]

Spector I, Shochet NR, Blasberger D, Kashman Y. Latrunculins--novel marine macrolides that disrupt microfilament organization and affect cell growth: I. Comparison with cytochalasin D. Cell Motil Cytoskeleton. 1989; 13:127–144. [PubMed: 2776221]

Spillane M, Ketschek A, Donnelly CJ, Pacheco A, Twiss JL, Gallo G. Nerve growth factor-induced formation of axonal filopodia and collateral branches involves the intra-axonal synthesis of regulators of the actin-nucleating Arp2/3 complex. J Neurosci. 2012; 32:17671–17689. [PubMed: 23223289]

Spillane M, Ketschek A, Jones SL, Korobova F, Marsick B, Lanier L, Svitkina T, Gallo G. The actin nucleating Arp2/3 complex contributes to the formation of axonal filopodia and branches through the regulation of actin patch precursors to filopodia. Dev Neurobiol. 2011; 71:747–758. [PubMed: 21557512]

Spillane M, Ketschek A, Merianda TT, Twiss JL, Gallo G. Mitochondria coordinate sites of axon branching through localized intra-axonal protein synthesis. Cell Rep. 2013; 5:1564–1575. [PubMed: 24332852]

Steketee MB, Moysidis SN, Weinstein JE, Kreymerman A, Silva JP, Iqbal S, Goldberg JL. Mitochondrial dynamics regulate growth cone motility, guidance, and neurite growth rate in perinatal retinal ganglion cells in vitro. Invest Ophthalmol Vis Sci. 2012; 53:7402–7411. [PubMed: 23049086]

Stokin GB, Lillo C, Falzone TL, Brusch RG, Rockenstein E, Mount SL, Raman R, Davies P, Masliah E, Williams DS, Goldstein LS. Axonopathy and transport deficits early in the pathogenesis of Alzheimer's disease. Science. 2005; 307:1282–1288. [PubMed: 15731448]

Tan SC, Scherer J, Vallee RB. Recruitment of dynein to late endosomes and lysosomes through light intermediate chains. Molecular biology of the cell. 2011; 22:467–477. [PubMed: 21169557]

Tang Y, Scott D, Das U, Gitler D, Ganguly A, Roy S. Fast vesicle transport is required for the slow axonal transport of synapsin. J Neurosci. 2013; 33:15362–15375. [PubMed: 24068803]

Tao K, Matsuki N, Koyama R. AMP-activated protein kinase mediates activity-dependent axon branching by recruiting mitochondria to axon. Dev Neurobiol. 2014; 74:557–573. [PubMed: 24218086]

Trushina E, Dyer RB, Badger JD 2nd, Ure D, Eide L, Tran DD, Vrieze BT, Legendre-Guillemin V, McPherson PS, Mandavilli BS, Van Houten B, Zeitlin S, McNiven M, Aebersold R, Hayden M, Parisi JE, Seeberg E, Dragatsis I, Doyle K, Bender A, Chacko C, McMurray CT. Mutant huntingtin impairs axonal trafficking in mammalian neurons in vivo and in vitro. Mol Cell Biol. 2004; 24:8195–8209. [PubMed: 15340079]

Uchida A, Alami NH, Brown A. Tight functional coupling of kinesin-1A and dynein motors in the bidirectional transport of neurofilaments. Mol Biol Cell. 2009; 20:4997–5006. [PubMed: 19812246]

Vale RD. The molecular motor toolbox for intracellular transport. Cell. 2003; 112:467–480. [PubMed: 12600311]

Vallee RB, McKenney RJ, Ori-McKenney KM. Multiple modes of cytoplasmic dynein regulation. Nature cell biology. 2012; 14:224–230.

Williamson TL, Cleveland DW. Slowing of axonal transport is a very early event in the toxicity of ALS-linked SOD1 mutants to motor neurons. Nat Neurosci. 1999; 2:50–56. [PubMed: 10195180]

Ye Y, Meyer HH, Rapoport TA. The AAA ATPase Cdc48/p97 and its partners transport proteins from the ER into the cytosol. Nature. 2001; 414:652–656. [PubMed: 11740563]

Yi J, Wu X, Chung AH, Chen JK, Kapoor TM, Hammer JA. Centrosome repositioning in T cells is biphasic and driven by microtubule end-on capture-shrinkage. J Cell Biol. 2013; 202:779–792. [PubMed: 23979719]

Yi JY, Ori-McKenney KM, McKenney RJ, Vershinin M, Gross SP, Vallee RB. High-resolution imaging reveals indirect coordination of opposite motors and a role for LIS1 in high-load axonal transport. J Cell Biol. 2011; 195:193–201. [PubMed: 22006948]

Yonekawa Y, Harada A, Okada Y, Funakoshi T, Kanai Y, Takei Y, Terada S, Noda T, Hirokawa N. Defect in synaptic vesicle precursor transport and neuronal cell death in KIF1A motor protein-deficient mice. J Cell Biol. 1998; 141:431–441. [PubMed: 9548721]

Yu W, Ahmad FJ, Baas PW. Microtubule fragmentation and partitioning in the axon during collateral branch formation. J Neurosci. 1994; 14:5872–5884. [PubMed: 7931550]

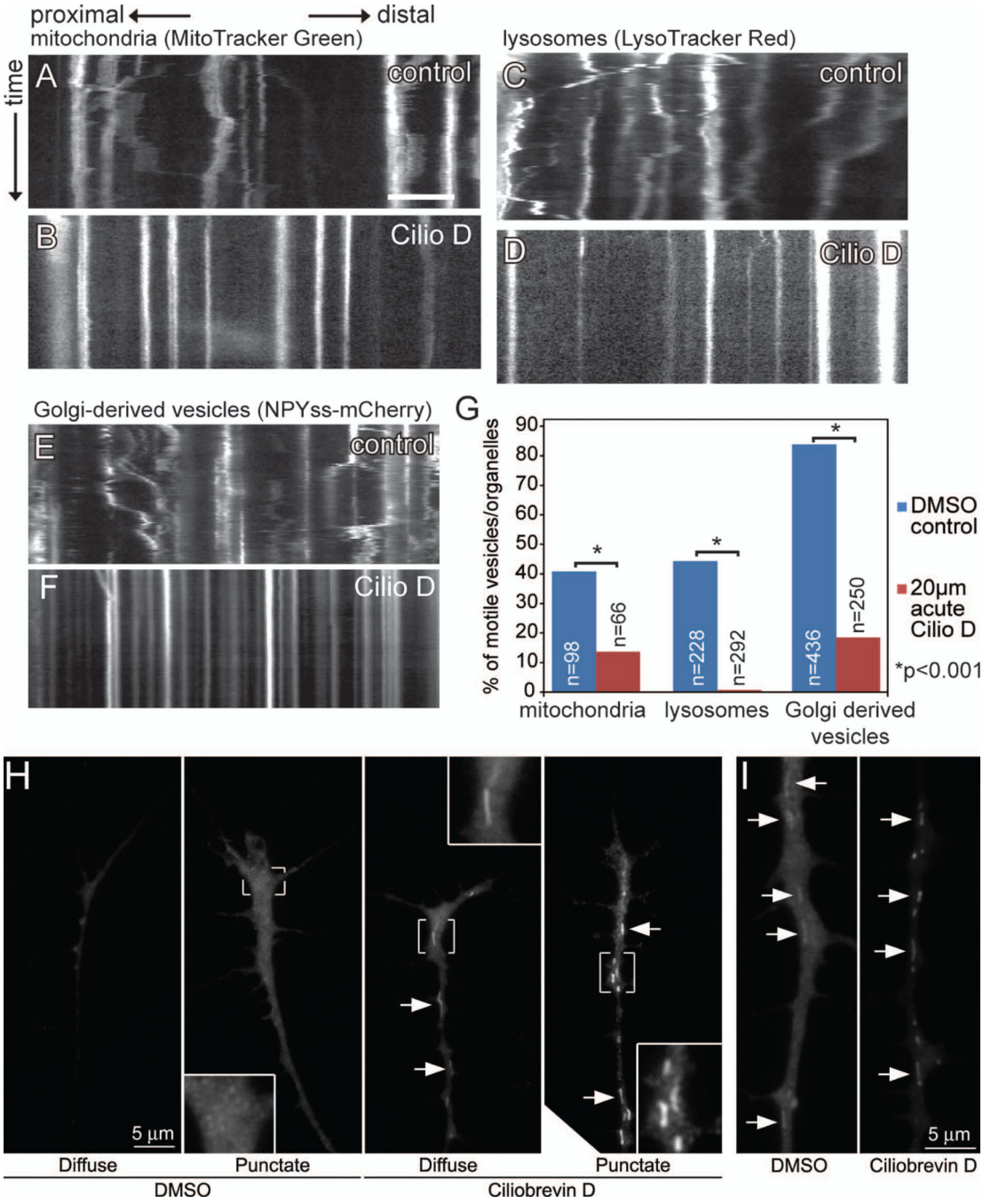

Figure 1.

Ciliobrevin D inhibits both anterograde and retrograde organelle transport and induces redistribution of p150 dynactin in axons. **(A)** Kymograph of mitochondrial movement along the axon. Mitochondria exhibit saltatory movement in both directions. X axis is the position along the axon shaft, with proximal movement (retrograde) going left and distal (anterograde) to the right. Y axis is time. Scale bar indicates 10µm. **(B)** A 45 minute incubation in 20 µM Ciliobrevin D inhibits mitochondrial movement both retrogradely and anterogradely. **(C)** Kymograph of lysosome movement, exhibiting largely retrograde

movement. **(D)** A 45 minute incubation in 20 μM Ciliobrevin D inhibits almost all lysosome movement. **(E)** Kymograph of Golgi-derived vesicle movement. Vesicles labeled by the NPYss-mCherry construct exhibit both anterograde and retrograde movement. **(F)** A 45 minute incubation in 20 μM Ciliobrevin D inhibits Golgi-derived vesicle movement. **(G)** Ciliobrevin D significantly reduces motility as revealed by quantification of the percent of motile vesicles (12 and 11 axons sampled for controls and CilioD groups), lysosomes (18 and 23 axons sampled for control and Cilio D groups) and mitochondria (8 and 6 axons sampled for controls and CilioD groups). **(H)** Examples of the distribution of p150 dynactin staining in axons treated with DMSO or Ciliobrevin D (20 μM, 30 min). In both panels H and I images in panels were acquired with identical settings and similarly processed. Arrows denote linear profiles. **(I)** Examples of linear profiles (arrows) staining with p150 dynactin antibodies exhibited greater intensities in Ciliobrevin D treated axons than DMSO treated.

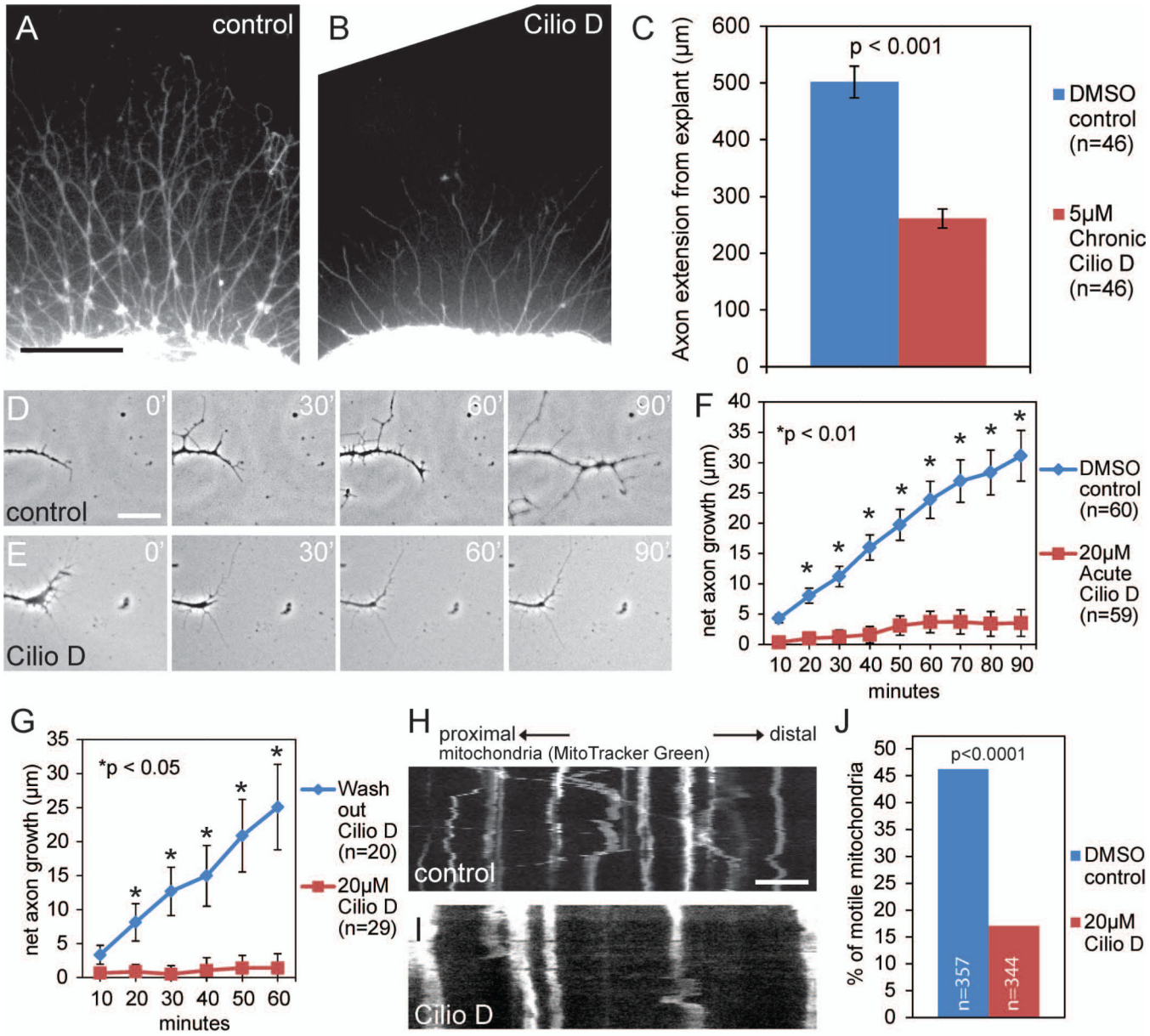

Figure 2.

Ciliobrevin D reversibly inhibits axon extension. **(A)** Phase contrast image of a representative DRG explant cultured overnight in NGF and DMSO (control). The sample is stained with anti-α-tubulin. Scale bar indicates 200μm. **(B)** Example of an explant cultured overnight in the continuous presence of 5μM Ciliobrevin D. Ciliobrevin D reduced axonal outgrowth (compare to panel A). **(C)** Quantification of the average distance control or Ciliobrevin D incubated axons extended from the explant when cultured overnight. Chronic Ciliobrevin D significantly reduces axonal outgrowth ($p<0.001$). **(D)** Phase contrast time-lapse sequence of DRG axon extension over 90 minutes after exposure to DMSO control media. Scale bar indicates 25μm. **(E)** Acute Ciliobrevin D treatment inhibits axon extension within 20 minutes of exposure. **(F)** Quantification of the net distance axons traveled within 90 minutes following exposure to DMSO control or acute Ciliobrevin D (treatment begins at

0 min). **(G)** Quantification of net axon extension in cultures initially incubated in Ciliobrevin D for 60 minutes, followed by wash out of the Cilibrevin D containing medium, and replacement with either Ciliobrevin D or DMSO containing medium at 0 min relative to the graph. **(H)** Kymograph of mitochondrial movement in axons after 20 a minute incubation in DMSO control. Scale bar indicates 10μm. **(I)** As in panel H, a kymograph of axonal mitochondria following 20 minute exposure to Ciliobrevin D. Note that compared to DMSO (H), the mitochondria in axons that were treated with Ciliobrevin D exhibit minimal motility. **(J)** Quantification of the percentage of motile mitochondria 20 min following incubation in Ciliobrevin D or DMSO containing media. Mitochondria were sampled from 8 and 5 axons in control and Ciliobrevin D groups, respectively, from the same number of cultures.

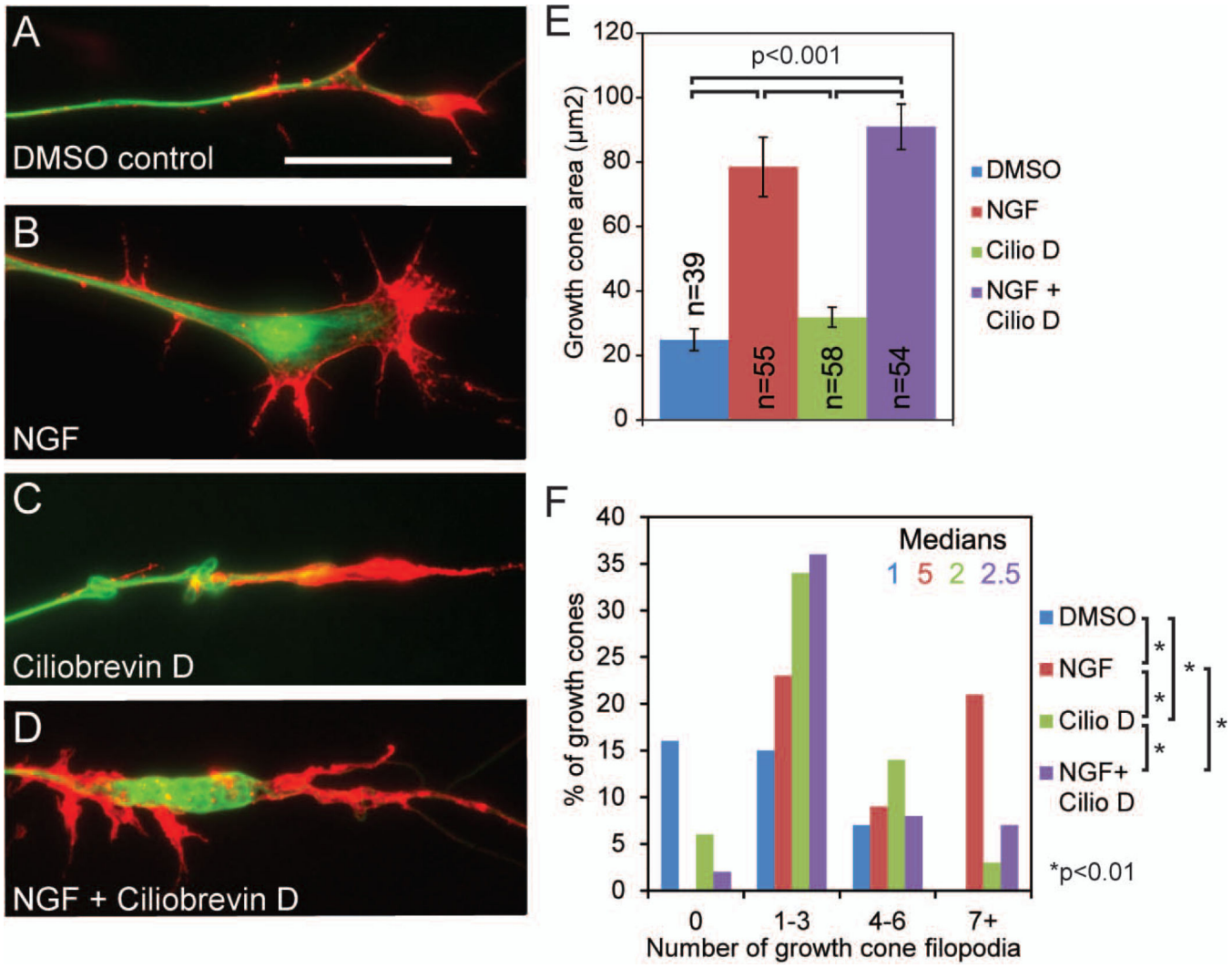

Figure 3.

Ciliobrevin D prevents NGF induced increases in the number of filopodia at growth cones but not the increase in growth cone area. **(A)** Example of the growth cone of an axon extending from a DRG explant cultured in the absence of NGF after a 40 minute exposure to DMSO control media with no NGF. The axon was simultaneously fixed and extracted, and stained to reveal actin filaments (red) and microtubules (green) (fixation and labeling scheme applies to panels A-D). Scale bar indicates 20µm. **(B)** Representative example of an axon with expanded growth cone after 40 minute exposure to NGF (40ng/ml). **(C)** Example of the growth cone of an axon following a 40 minute treatment with 20 µM Ciliobrevin D in the absence of further treatment with NGF. **(D)** Example of a growth cone after 40 minute exposure to both Ciliobrevin D and NGF. Note the reduced number of filopodia compared to panel B (NGF treatment) but the maintenance of the NGF-induced increase in area (compare to panel C). **(E)** Quantification of growth cone area. Ciliobrevin D, does not prevent the NGF dependent growth cone expansion. n=growth cones sampled from 4-6 cultures. **(F)** Distribution of the percentage of growth cones exhibiting the binned number of filopodia. Ciliobrevin D treatment alone increased the number of filopodia at growth cones relative to

DMSO controls, but Ciliobrevin D treatment failed to elicit any additional increases in the number of filopodia in the presence of NGF, and instead reduced the number of growth cone filopodia. Filopodia were analyzed in the same set of growth cones as in panel E.

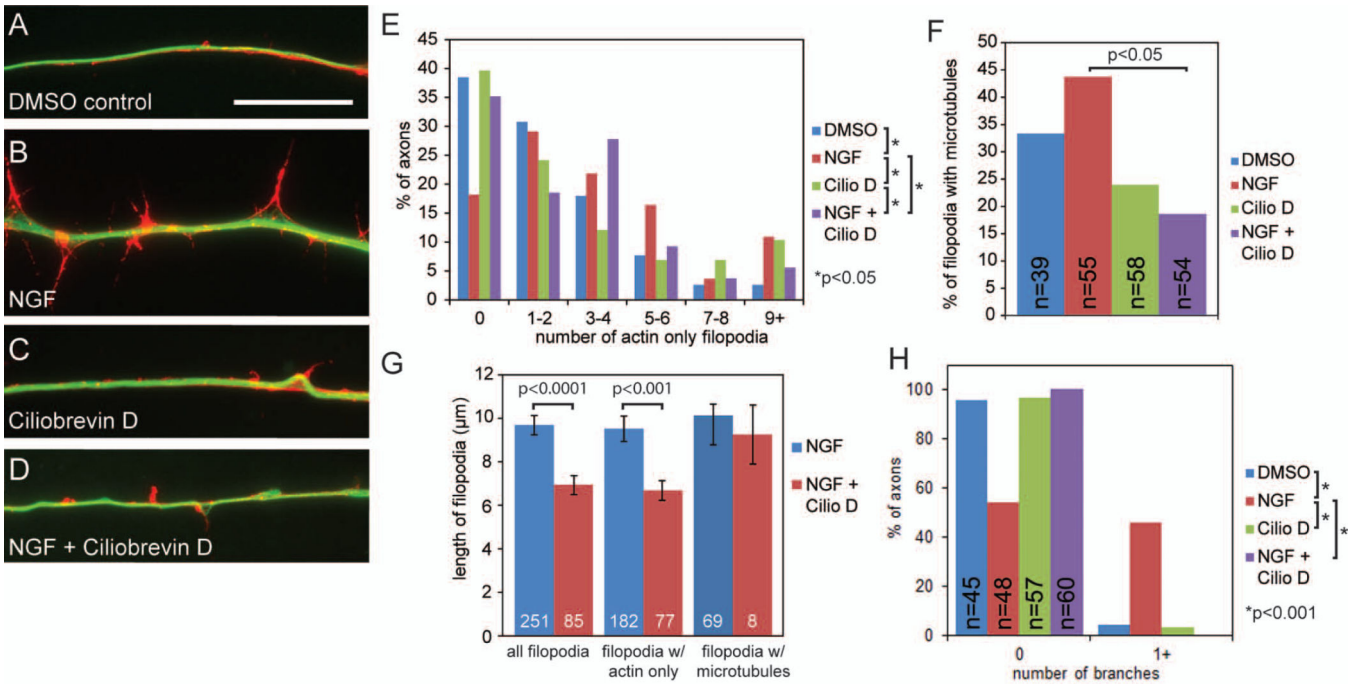

Figure 4.

Ciliobrevin D inhibits NGF induced increases in the number of axonal filiopodia and branches. **(A)** Example of an axonal filopodia containing actin filaments (red) and filopodia containing microtubules (green) in cultures after 40 minute exposure to DMSO control media (samples were fixed and stained as in Figure 3). Scale bar indicates 20 μm. **(B)** Example of an axon with increased axonal filopodia number and length after a 40 minute treatment with NGF (40ng/ml). **(C)** Example of an axon following a 40 minute treatment with 20 μM Ciliobrevin D. **(D)** Example of an axon following a 40 minute treatment with both 20 μM Ciliobrevin D and NGF displaying reduced axonal filopodia compared to axons treated with NGF alone (panel B). **(E)** Distribution of the percentage of axons that contained the binned number of filopodia containing only actin filaments and not microtubules. Ciliobrevin D reduces the number filopodia containing only actin filaments. 39-54 axons were sampled from 3-6 cultures per group. **(F)** Quantification of the percentage of axonal filopodia that contain microtubules, presented as the percentage of all filopodia present along the axons sampled in panel E. NGF promotes the targeting of microtubules into axonal filopodia, and Ciliobrevin D treatment decreases the number of filopodia containing microtubules following treatment with NGF. Analysis performed using Chi-squared tests. **(G)** Quantification of the length of all axonal filopodia, filopodia containing only actin filaments or filopodia with both actin and microtubules. **(H)** Quantification of the percent of axons that display at least one branch. NGF induces formation of branches, which is prevented by Ciliobrevin D.

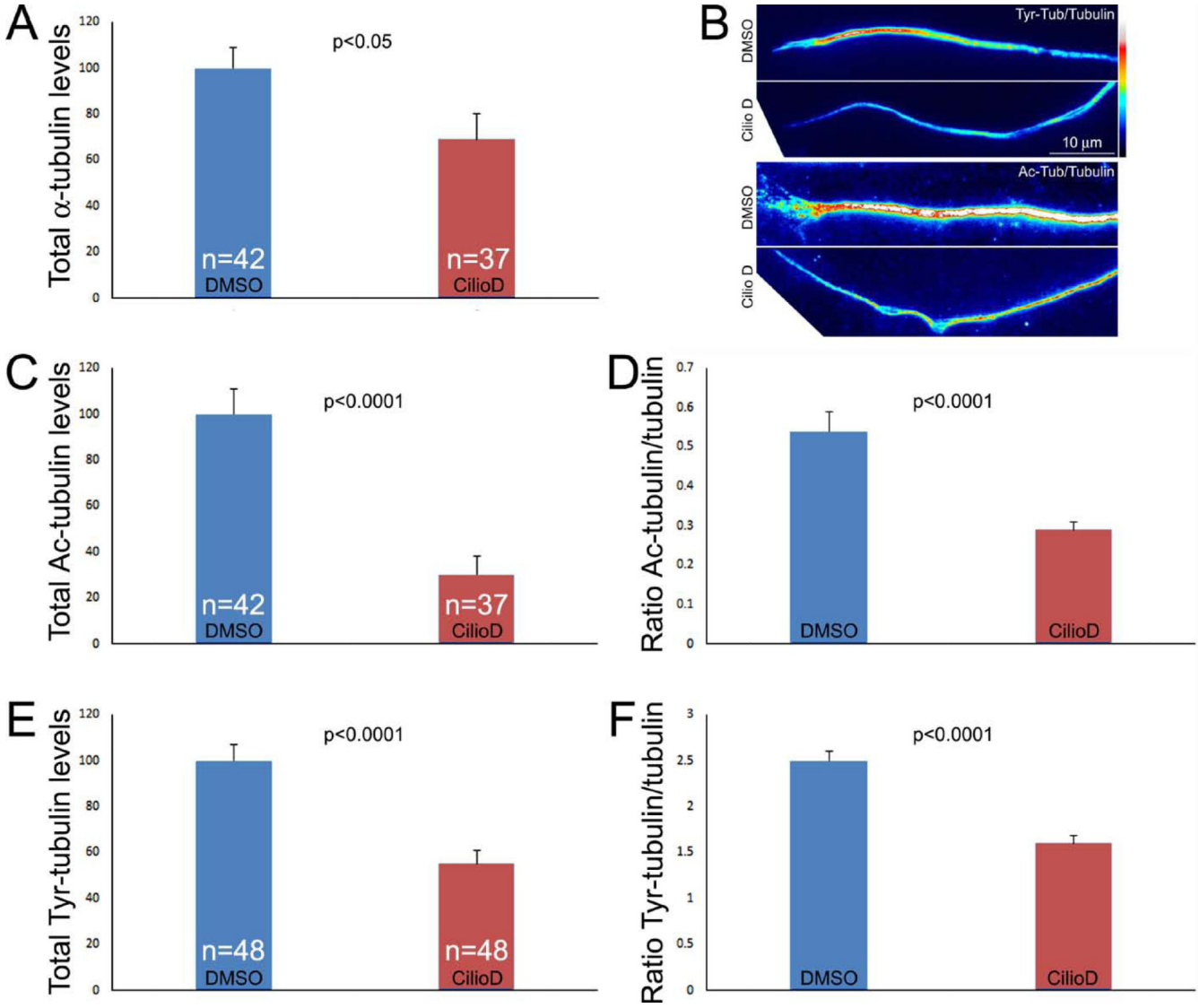

Figure 5.

Effects of Ciliobrevin D on tubulin post-translational modifications. **(A)** Graph showing the absolute values of the integrated intensities of total α-tubulin in the distal 50 µm of axons. n=axons sampled from 4-6 cultures per group. **(B)** Examples of representative ratiometric images reflective of the ratios of acetylated (Ac) and tyrosinated (Tyr) tubulin to total α-tubulin (images prepared using Image J ratiometric plugin). Ciliobrevin D decreased the ratios of both tubulin modifications to total tubulin. **(C)** Graph of the total levels of acetylated tubulin in the distal 50 µm of axons, normalized to DMSO treatment. **(D)** Graph showing the ratiometric values of acetylated tubulin to total tubulin levels. **(E)** Graph of the total levels of tyrosinated tubulin in the distal 50 µm of axons, normalized to DMSO treatment. **(F)** Graph showing the ratiometric values of tyrosinated tubulin to total tubulin levels.

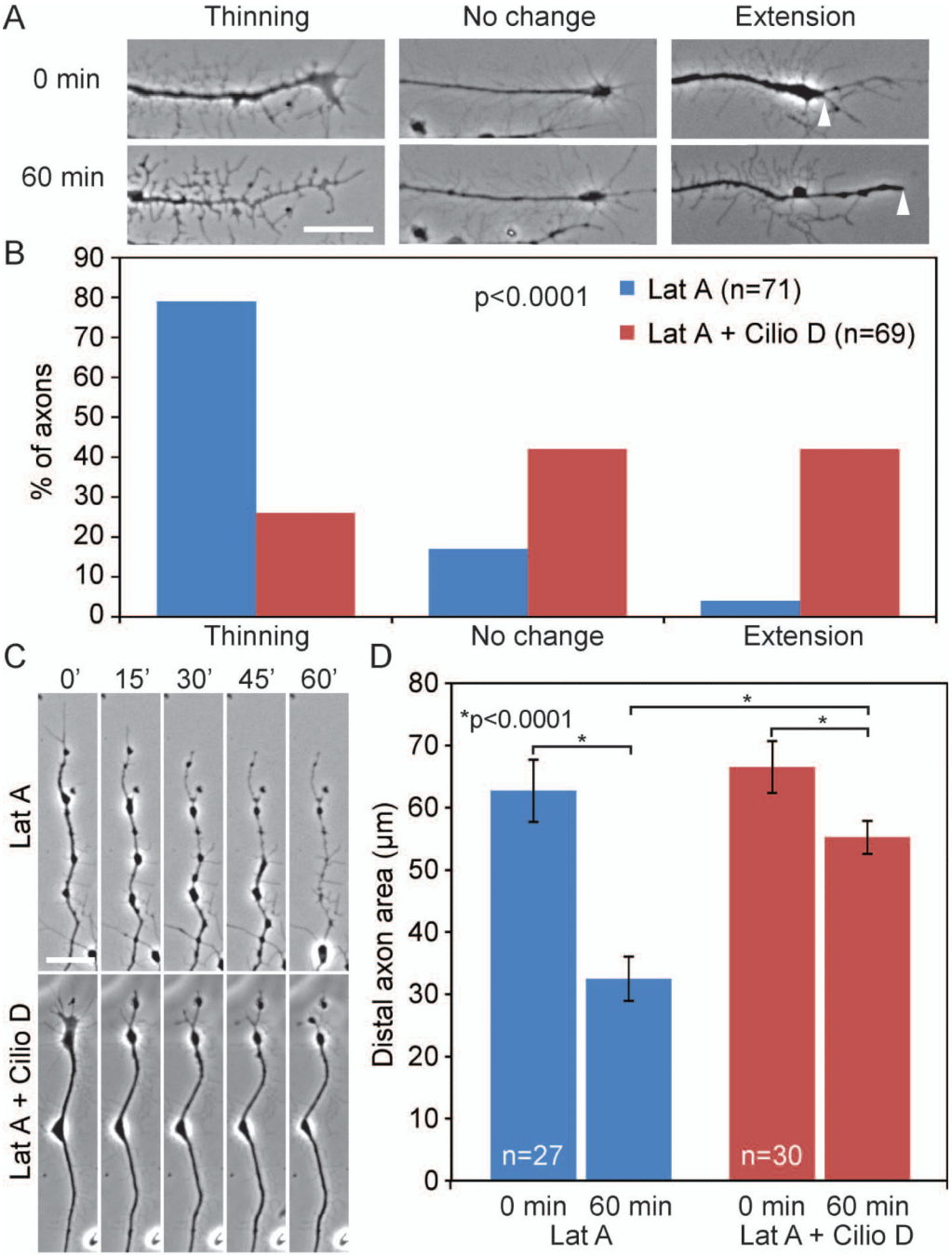

Figure 6.

Ciliobrevin D minimizes latrunculin A (LatA) induced retrograde cytoplasmic redistribution. **(A)** Examples of the three categories used for semi-quantitative analysis of the effects of 5 µM LatA treatment on the appearance of distal axons. Note the phase contrast light appearance of the distal axon in the "thinning" category at 60 min of LatA treatment compared to 0 min. Arrowheads in the extension category denote the distal most extent of the phase dark component of the axon at 0 and 60 min respectively. **(B)** Semi-quantitative analysis of the response of axons to a 1 hr treatment with 5 µM LatA. Axons

were categorized based on their morphology at 60 min post-treatment relative to immediately after treatment. n=number of axons shown in the bars sampled from 6 cultures per group. LatA treatment induced thinning of the axons. Cotreatment with 20 μM Ciliobrevin D greatly attenuated axon thinning and promoted distal axon extension. **(C)** Representative stills from time-lapse sequences showing the retrograde redistribution of cytoplasm in the distal axons following LatA treatment (top panels) and the impairment of this redistribution by cotreatment with Ciliobrevin D. **(D)** Quantitative analysis of the area of the distal 40 μm of axons at 0 and 60 min post-treatment. In axons not exhibiting extension, the area of the axon was measured from the point demarcating 40 μm behind the axon tip at time 0 min. In axons exhibiting extension, the measurement was made from the point demarcating 40 μm behind the axon tip at time 0 and 60 min respectively. The initial area measurements at 0 min did not differ between the LatA and LatA + Ciliobrevin D groups. LatA treatment decreased axon area, and Ciliobrevin D cotreatment strongly attenuated the decrease in axon area. Axons sampled from 4 cultures per group.

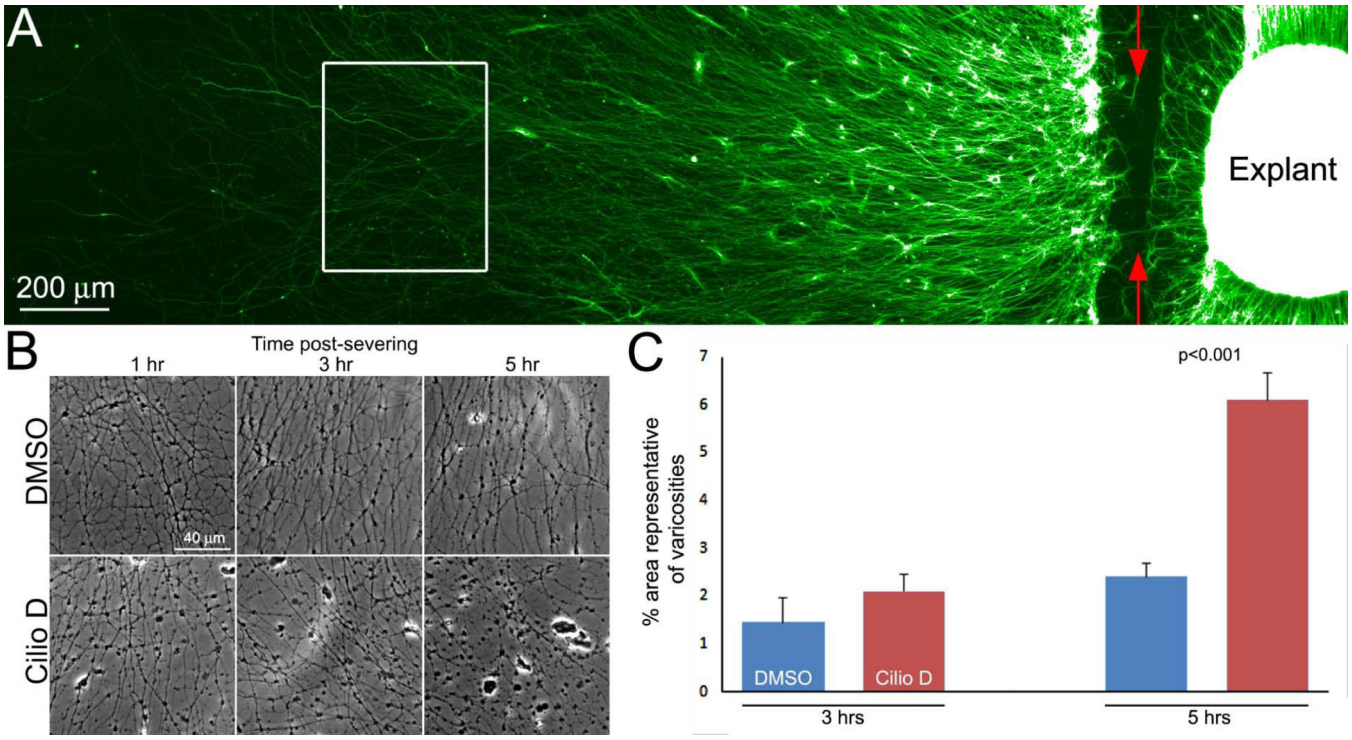

Figure 7.

Ciliobrevin D promotes the degeneration of the distal axon after severing. **(A)** Example of an explant stained with anti-tubulin to reveal axons denoting the site of severing (red arrows) and a representative region where the images in later panels were sampled (white box). **(B)** Phase contrast images of axons at 1-5 hrs post severing. Axonal varicosities increase with time after severing and appear as black beads along the axons. Ciliobrevin D treatment increased the presence of variocosities. The increased presence of varicosities was most pronounced at 5 hrs postsevering. **(C)** Graph showing the extent of varicosity formation along axons as an indicator of axon degeneration. As described in the Methods, the area of images representative of varicosities was determined for 9 explants from images of live axons taken using phase contrast imaging at 3 and 5 hrs post severing. The extent of varicosity formation in DMSO treated cultures increased between 3 and 5 hrs ($p=0.03$). Although the mean extent of varicosity formation in the presence of Ciliobrevin D was increased by 43% relative to DMSO treatment at 3 hrs post severing, this did not result in a significant difference in a Bonferroni multiple comparison test analysis. However, by 5 hrs varicosity formation was increased by 154% in Ciliobrevin D treated axons relative to DMSO controls ($p<0.001$).

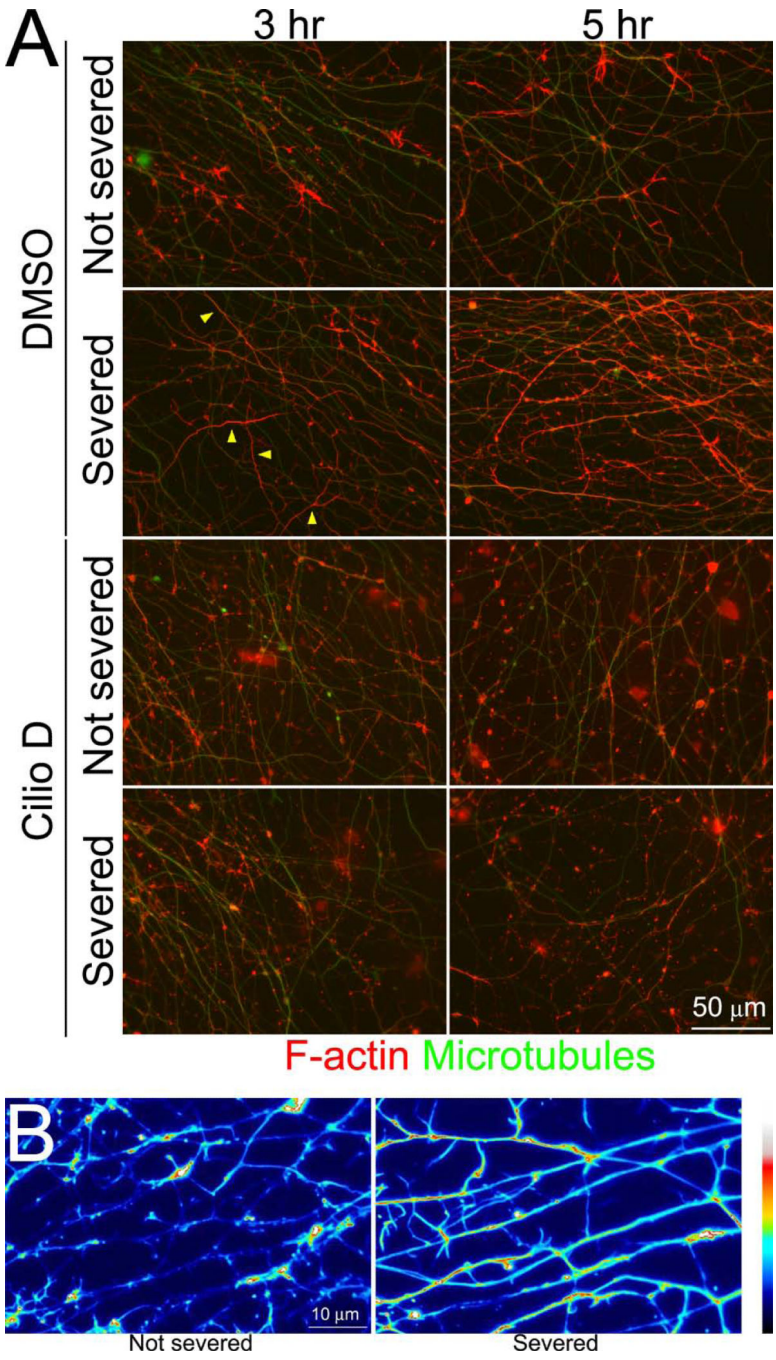

Figure 8.

Ciliobrevin D prevents axon severing induced changes in axonal actin organization. **(A)** Examples of axons that underwent combined fixation and extraction and were labeled to reveal microtubules and actin filaments. Not severed axons exhibit the normal distribution of axonal actin filaments, characterized by localized patches and accumulations amongst a low level of filaments. By 3 hrs following severing axons have begun to exhibit increased levels of actin filaments, which in some axons appear to fill the axon (examples denoted by yellow arrow). By 5 hrs the increase in actin filaments and filling of the axon in severed axons has

become more prominent and frequent. In cultured treated with Ciliobrevin D actin filaments did not fill axons and presented as patches and accumulations along the length of the axon. **(B)** False colored higher magnification examples of axons, severed or not severed, from control cultures at 5 hrs post severing. Note the relatively uniform distribution of actin filaments in severed axons.